NATIONAL ADVISORY COMMITTEE FOR AERONAUTICS

REPORT No. 683

CORRELATION OF COOLING DATA FROM AN AIR-COOLED CYLINDER AND SEVERAL MULTICYLINDER ENGINES

By BENJAMIN PINKEL and HERMAN H. ELLERBROCK, Jr.

1940

For sale by the Superintendent of Documents, Washington, D. C. - - - - - - - - - - - - - - - Price 10 cents
Subscription price, $3 per year

AERONAUTIC SYMBOLS

1. FUNDAMENTAL AND DERIVED UNITS

	Symbol	Metric		English	
		Unit	Abbreviation	Unit	Abbreviation
Length	l	meter	m	foot (or mile)	ft. (or mi.)
Time	t	second	s	second (or hour)	sec. (or hr.)
Force	F	weight of 1 kilogram	kg	weight of 1 pound	lb.
Power	P	horsepower (metric)		horsepower	hp.
Speed	V	kilometers per hour	k.p.h.	miles per hour	m.p.h.
		meters per second	m.p.s.	feet per second	f.p.s.

2. GENERAL SYMBOLS

W, Weight $=mg$

g, Standard acceleration of gravity $=9.80665$ m/s^2 or 32.1740 ft./sec.^{2}

m, Mass $=\frac{W}{g}$

I, Moment of inertia $=mk^2$. (Indicate axis of radius of gyration k by proper subscript.)

μ, Coefficient of viscosity

ν, Kinematic viscosity

ρ, Density (mass per unit volume)

Standard density of dry air, 0.12497 kg-m^{-4}-s^2 at 15° C. and 760 mm; or 0.002378 lb.-ft.$^{-4}$ sec.^{2}

Specific weight of "standard" air, 1.2255 kg/m^3 or 0.07651 lb./cu. ft.

3. AERODYNAMIC SYMBOLS

S, Area

S_w, Area of wing

G, Gap

b, Span

c, Chord

$\frac{b^2}{S}$, Aspect ratio

V, True air speed

q, Dynamic pressure $=\frac{1}{2}\rho V^2$

L, Lift, absolute coefficient $C_L=\frac{L}{qS}$

D, Drag, absolute coefficient $C_D=\frac{D}{qS}$

D_0, Profile drag, absolute coefficient $C_{D_0}=\frac{D_0}{qS}$

D_i, Induced drag, absolute coefficient $C_{D_i}=\frac{D_i}{qS}$

D_p, Parasite drag, absolute coefficient $C_{D_p}=\frac{D_p}{qS}$

C, Cross-wind force, absolute coefficient $C_C=\frac{C}{qS}$

R, Resultant force

i_w, Angle of setting of wings (relative to thrust line)

i_t, Angle of stabilizer setting (relative to thrust line)

Q, Resultant moment

Ω, Resultant angular velocity

$\rho\frac{Vl}{\mu}$, Reynolds Number, where l is a linear dimension (e.g., for a model airfoil 3 in. chord, 100 m.p.h. normal pressure at 15° C., the corresponding number is 234,000; or for a model of 10 cm chord, 40 m.p.s., the corresponding number is 274,000)

C_p, Center-of-pressure coefficient (ratio of distance of c.p. from leading edge to chord length)

α, Angle of attack

ϵ, Angle of downwash

α_0, Angle of attack, infinite aspect ratio

α_i, Angle of attack, induced

α_a, Angle of attack, absolute (measured from zero-lift position)

γ, Flight-path angle

REPORT No. 683

CORRELATION OF COOLING DATA FROM AN AIR-COOLED CYLINDER AND SEVERAL MULTICYLINDER ENGINES

By BENJAMIN PINKEL and HERMAN H. ELLERBROCK, Jr.

Langley Memorial Aeronautical Laboratory

NATIONAL ADVISORY COMMITTEE FOR AERONAUTICS

HEADQUARTERS, NAVY BUILDING, WASHINGTON, D. C.

LABORATORIES, LANGLEY FIELD, VA.

Created by act of Congress approved March 3, 1915, for the supervision and direction of the scientific study of the problems of flight (U. S. Code, Title 50, Sec. 151). Its membership was increased to 15 by act approved March 2, 1929. The members are appointed by the President, and serve as such without compensation.

GEORGE W. LEWIS, *Director of Aeronautical Research* S. PAUL JOHNSTON, *Coordinator of Research*

JOHN F. VICTORY, *Secretary*

HENRY J. E. REID, *Engineer in Charge, Langley Memorial Aeronautical Laboratory, Langley Field, Va.*

JOHN J. IDE, *Technical Assistant in Europe, Paris, France*

TECHNICAL COMMITTEES

AERODYNAMICS
POWER PLANTS FOR AIRCRAFT
AIRCRAFT MATERIALS

AIRCRAFT STRUCTURES
AIRCRAFT ACCIDENTS
INVENTIONS AND DESIGNS

Coordination of Research Needs of Military and Civil Aviation

Preparation of Research Programs

Allocation of Problems

Prevention of Duplication

Consideration of Inventions

LANGLEY MEMORIAL AERONAUTICAL LABORATORY

LANGLEY FIELD, VA.

Unified conduct, for all agencies, of scientific research on the fundamental problems of flight.

OFFICE OF AERONAUTICAL INTELLIGENCE

WASHINGTON, D. C.

Collection, classification, compilation, and dissemination of scientific and technical information on aeronautics.

4-1-40

REPORT No. 683

CORRELATION OF COOLING DATA FROM AN AIR-COOLED CYLINDER AND SEVERAL MULTICYLINDER ENGINES

By Benjamin Pinkel and Herman H. Ellerbrock, Jr.

SUMMARY

The theory of engine-cylinder cooling developed in a previous report was further substantiated by data obtained on a cylinder from a Wright R–1820–G engine. Equations are presented for the average head and barrel temperatures of this cylinder as functions of the engine and the cooling conditions. These equations are utilized to calculate the variation in cylinder temperature with altitude for level flight and climb. A method is presented for correlating average head and barrel temperatures and temperatures at individual points on the head and the barrel obtained on the test stand and in flight. The method is applied to the correlation and the comparison of data obtained on a number of service engines. Data are presented showing the variation of cylinder temperature with time when the power and the cooling pressure drop are suddenly changed.

INTRODUCTION

An analysis has been reported (reference 1) of the heat-transfer processes of an air-cooled engine for the purpose of determining the manner in which the various engine and cooling conditions combine to determine the cylinder temperature. The average head and barrel temperatures were each given as a simple function of the important conditions, making it possible to correct cylinder temperatures of a given engine for variation in engine power, air-fuel ratio, mass flow of cooling air, and atmospheric temperature. Tests were made on a cylinder from a Pratt & Whitney R–1535 engine and on a cylinder from a Pratt & Whitney R–1340–H engine to check the analysis and to provide the experimental constants in the equations for the average head and barrel temperatures as functions of the fundamental engine and cooling variables.

The present report is a continuation of the foregoing research. Data on a cylinder from a Wright R–1820–G engine are used to provide an additional check of the analysis given in reference 1 and to provide the necessary constants for this cylinder.

The method presented for correlating engine-temperature data is applied to obtain a comparison of the cooling of several engines on the test stand and in flight.

A discussion is given of the variation in temperature around the cylinder and a method of correlating cylinder temperatures at individual points is presented. This method is illustrated by applying it to the correlation of data for the Wright R–1820–G engine.

The variation of engine temperature with altitude (from sea level to 30,000 feet) for the conditions of level flight and climb at constant indicated air speed are calculated from the equations obtained for the cooling of the Wright R–1820–G engine.

194665—40——1

NOTATION

$a = U_x/(U_x+q_{0_x})$.

a_0, outside-wall area of head of cylinder covered by fins, square inches.

a_1, inside-wall area of head of cylinder, square inches.

A_c, cross-sectional area of piston, square inches.

$b = q_{0_x}/(U_x+q_{0_x})$.

B and $\overline{B}$, constants.

c, specific heat of metal in cylinder head, B. t. u. per pound per °F.

c_p, specific heat of air at constant pressure, B. t. u. per pound per °F.

H, heat transferred per unit time from combustion gases to cylinder head, B. t. u. per hour.

H_1, heat transferred per unit time from cylinder head to cooling air, B. t. u. per hour.

H_h, theoretical heat transferred per unit time from one side of cylinder per unit height, B. t. u. per hour per inch.

I, indicated horsepower per cylinder.

k_m, thermal conductivity of metal in cylinder head, B. t. u. per square inch per °F. per hour through 1 inch.

K, K_1, m, n, and n', constants for a given air-flow condition and engine.

M, effective weight of cylinder head, pounds.

q_1, surface heat-transfer coefficient from combustion gases to inside of cylinder wall of engine, B. t. u. per square inch per °F. per hour.

q_0, heat-transfer coefficient from combustion gases to outside of cylinder wall of engine based on average wall temperature, B. t. u. per square inch per °F. per hour.

q_{0_x}, local heat-transfer coefficient from combustion gases to outside cylinder wall, B. t. u. per square inch per °F. per hour.

t, time, hours.

t', time, minutes.

t_w, thickness of cylinder-head wall, inches.

T_{a_x}, local cooling-air temperature around cylinder, °F.

T_{a_1}, inlet temperature of cooling air, °F.

T_b, average temperature over outside cylinder-barrel surface when equilibrium is attained, °F.

T_g, effective gas temperature, °F.

T_h, average temperature over outside cylinder-head surface when equilibrium is attained, °F.

$T_{a_{av}}$, average temperature of cooling air, °F.

T_{a_0}, outlet cooling-air temperature, °F.

T_{g_x}, local effective gas temperature, °F.

T_{h_i}, average temperature over inside cylinder-head surface when equilibrium is attained, °F.

T_{h_0}, average temperature of cylinder head at time $t=0$, °F.

T_{h_t}, average temperature of cylinder head at time t, °F.

T_{h_x}, local cylinder-head temperature, °F.

U, over-all heat-transfer coefficient from outside cylinder wall of engine to cooling air based on difference between average cylinder temperature and inlet cooling-air temperature, B. t. u. per square inch per °F. per hour.

U_{av}, average over-all heat-transfer coefficient from outside cylinder wall of engine to cooling air based on difference between average cylinder temperature and average cooling-air temperature, B. t. u. per square inch per °F. per hour.

U_x, local heat-transfer coefficient from outside cylinder wall to cooling air, B. t. u. per square inch per °F. per hour.

V, velocity of cooling-air stream, feet per second.

v, displacement volume of cylinder, cubic inches.

W, weight of cooling air flowing around cylinder per unit time, pounds per second.

W_h, weight of cooling air flowing around cylinder per unit time per unit height, pounds per hour per inch.

W_t, product of weight of gases in cylinder and number of cycles per unit time, pounds per minute.

x, variable circumferential distance from front of cylinder, inches.

x_t, circumferential distance from front to rear of cylinder, inches.

ρ, average density of cooling air entering and leaving fins, pound-second ^{2} per foot ^{4}.

ρ_0, density of air at 29.92 inches of mercury and 70° F., pound-second ^{2} per foot ^{4}.

ρ_{SL}, density of air at 29.92 inches of mercury and 59° F., pound-second ^{2} per foot ^{4}.

Δp, pressure drop across cylinder, inches of water (includes loss caused by expansion of air from exit of baffle).

Δp_{SL}, pressure drop across cylinder at standard sea-level conditions, inches of water.

ANALYSIS

AVERAGE CYLINDER TEMPERATURE

Average cylinder temperature as a function of engine and cooling conditions.—As a starting point in the analysis, the equations for the transfer of heat from the combustion gases to the engine cylinder and from the cylinder to the cooling air will be reviewed. The rate of heat transfer from the combustion gases to the cylinder head may be written, as a good first approximation (reference 1)

$$H=Ba_1W_t^n(T_g-T_h) \tag{1}$$

In the range of air-fuel ratios to the rich side of the theoretically correct mixture, an equation similar to equation (1) but involving I instead of W_t is given by

$$H=\overline{B}a_1I^{n'}(T_g-T_h) \tag{2}$$

For the rate of heat transfer from the cylinder head to the cooling air, the following equation is given in reference 1:

$$H_1=Ka_0(\Delta p\rho/\rho_0)^m(T_h-T_{a_1}) \tag{3}$$

For equilibrium, the rate of heat transfer to the cylinder head is equal to the rate of heat transfer away from the cylinder head and, from equations (2) and (3), the following equation is obtained for T_h:

$$T_h=\frac{T_g-T_{a_1}}{\frac{Ka_0(\Delta p\rho/\rho_0)^m}{\overline{B}a_1I^{n'}}+1}+T_{a_1} \tag{4}$$

An equation similar to (4), but involving the weight of gas in the engine cylinder, may be obtained from equations (1) and (3). A set of equations similar to (1), (2), (3), and (4) may be written for the barrel. In the following analysis, equations will be given only for the head temperature and a parallel set will be understood to apply for the barrel temperature. As shown in reference 1, the effective temperature of the combustion gases T_g is dependent on the fuel-air ratio, the compression ratio, the carburetor-air temperature, and the spark setting; as a good first approximation, T_g is independent of the engine speed and the brake mean effective pressure.

An equation for T_g is set up in reference 1 in which a term for the weight of residuals appears but, in the search for a first approximation, this term is assumed to be negligible and is eliminated in the final equations. In order to check the error in this simplification, the value of T_g was obtained by tests in which the weight of residuals was varied by varying the exhaust back pressure.

Heat transfer through cylinder head.—The mean coefficient over the entire cycle for the transfer of heat from the combustion gases to the cylinder is defined in reference 1 as

$$q_0=\frac{H}{a_1(T_g-T_h)} \tag{5}$$

When equation (5) is compared with equation (1), the mean coefficient is seen to be also equal to BW_t^n. Because q_0 is based on outside-wall temperature T_h, it is an over-all heat-transfer coefficient taking into account the transfer of heat by convection from the gas to the inner wall and the transfer by conduction from the inner to the outer wall. The heat-transfer coefficient q_1 for convection of heat from the gas to the inner wall is given by

$$q_1=\frac{H}{a_1(T_g-T_{h_1})} \tag{6}$$

The conduction of heat through the head may be expressed by the following equation:

$$H=a_1\frac{k_m}{t_w}(T_{h_1}-T_h) \tag{7}$$

When equations (5), (6), and (7) are combined, the coefficient q_1 in terms of the over-all coefficient q_0 may be obtained,

$$q_1=\frac{q_0}{1-\frac{t_w}{k_m}q_0} \tag{8}$$

For a given engine, t_w and k_m are constant so that both q_1 and q_0 vary with the same engine conditions. The difference between q_1 and q_0 is small, as will be shown later.

Comparison of cooling of cylinders.—By rearrangement of terms, equation (4) may also be written

$$\frac{T_h-T_{a_1}}{T_g-T_h}=\frac{\overline{B}a_1I^{n'}}{Ka_0(\Delta p\rho/\rho_0)^m}=K_1\frac{I^{n'}}{(\Delta p\rho/\rho_0)^m} \tag{9}$$

The values of n' are approximately twice the values of m for cylinders that have been tested. Equation (9) may then be written as the approximation,

$$\frac{T_h-T_{a_1}}{T_g-T_h}=f\left[\frac{(I/v)^2}{(\Delta p\rho/\rho_0)}\right] \tag{10a}$$

Thus, when $(T_h-T_{a_1})/(T_g-T_h)$ is plotted against $(I/v)^2/(\Delta p\rho/\rho_0)$, a single curve should result for a given engine irrespective of the engine or the cooling condition varied. Curves of this type provide means of comparing the cooling of two engines, although the tests may not have been made at identical operating conditions. The lower the curve, the lower the cylinder-head temperature for a given specific indicated horsepower and cooling-pressure drop.

In some cases, the velocity V of the cooling-air stream rather than the pressure drop across the cylinder is known. Inasmuch as, for practical purposes, $V\rho/\rho_0$ is proportional to $(\Delta p\rho/\rho_0)^{1/2}$, it is evident that equation (10a) may be written in the form

$$\frac{T_h-T_{a_1}}{T_g-T_h}=f_1\left(\frac{I/v}{V\rho/\rho_0}\right) \tag{10b}$$

and the cooling data may be correlated by plotting $(T_h-T_{a_1})/(T_g-T_h)$ against $\frac{I/v}{V\rho/\rho_0}$ on logarithmic coordinates. As before, a single curve should result irrespective of engine or cooling conditions.

TEMPERATURE AT INDIVIDUAL POINTS ON CYLINDER

An analysis of the theoretical distribution of temperature around the cylinder is given in the appendix. (See equations (11) to (30).) Based on this analysis, the following equation is obtained for correlating the temperatures at individual points (see equation (30) and discussion in appendix):

$$\frac{(\Delta p\rho/\rho_0)^m}{I^{n'}}\frac{T_{h_x}-T_{a_1}}{T_{g_x}-T_{h_x}}=f_2(\Delta p\rho/\rho_0)$$

APPARATUS

The cylinder on which the tests were made was obtained from a Wright R–1820–G engine (fig. 1). The bore was 6⅛ inches, the stroke was 7 inches, and the compression ratio was 7.4. The cylinder, enclosed in a jacket through which cooling air was forced by a centrifugal blower, was mounted on a single-cylinder test stand. The jacket had a wide entrance section to provide a low air velocity over the front half of the cylinder; over the rear half, the jacket fitted closely against the fins to provide a high air velocity. The engine set-up is shown in figure 2.

A partition was located in the exit duct of the jacket for separating the air that flowed over the head from the air that flowed over the barrel. Thermocouples were located in the jacket ahead of the cylinder and in the exit passages from the head and the barrel for measuring the increase in temperature of the cooling air.

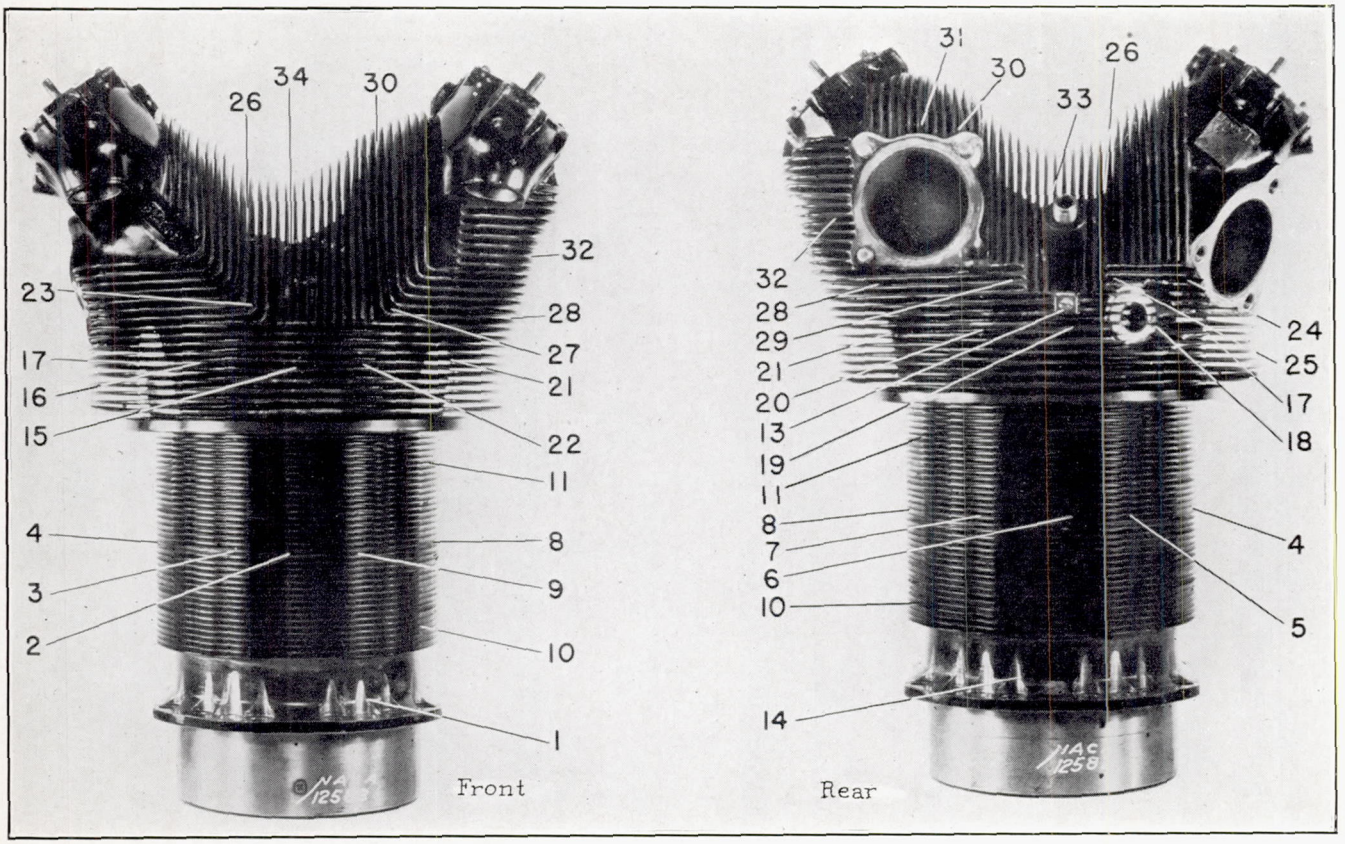

FIGURE 1.—The 1820–G cylinder showing location of thermocouples.

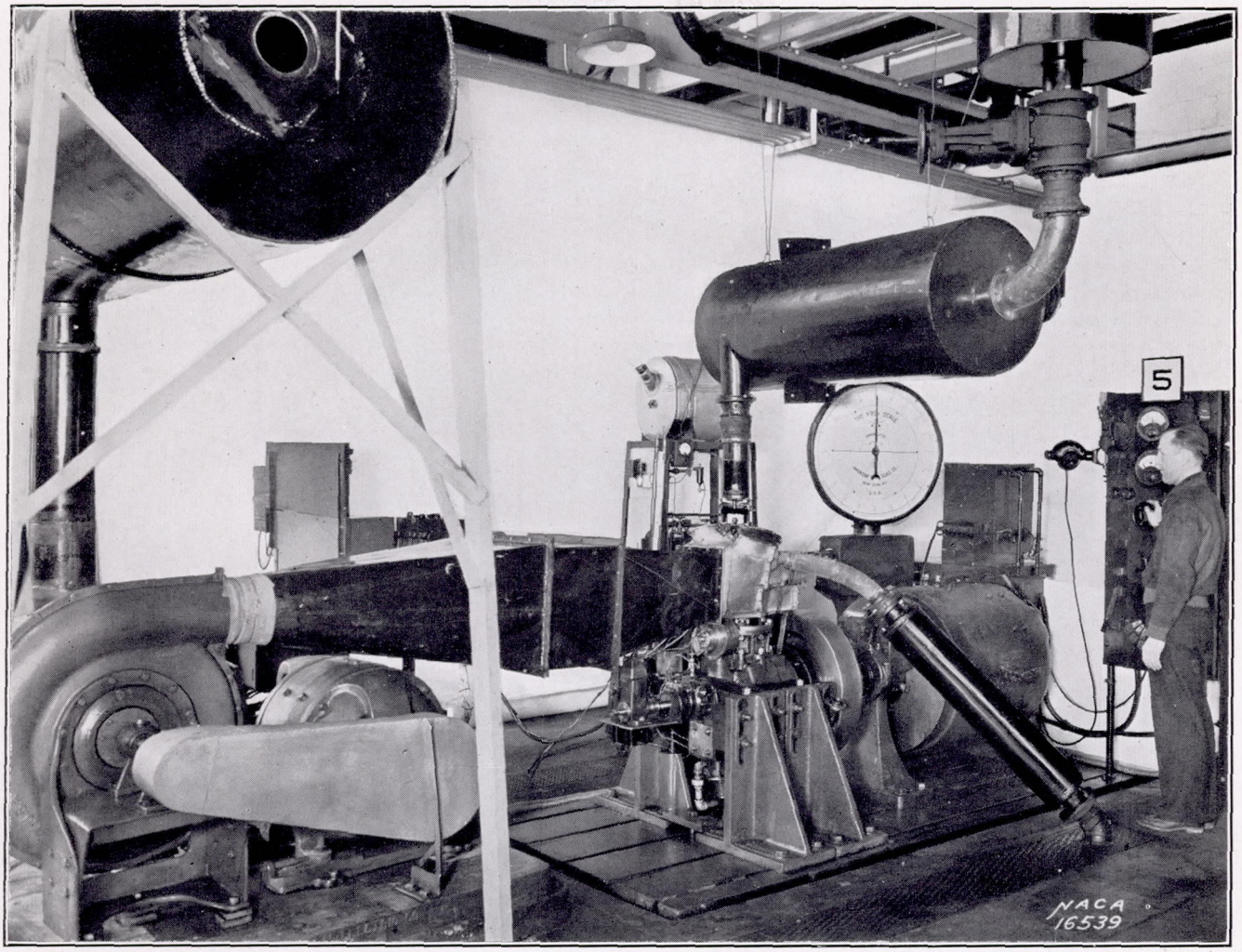

FIGURE 2.—Set-up of single-cylinder air-cooled engine.

The temperatures of the cylinder were measured by 22 thermocouples on the head, 10 on the barrel, and 2 on the flange.

The apparatus for measuring the pressure drop across the cylinder, the quantity of cooling air supplied to the jacket, and the fuel-air ratio is fully described in reference 1. Electrical heaters located in the air duct between the blower and the jacket were provided to vary the cooling-air temperature. Electrical heaters were also located in the intake system of the engine for varying the carburetor-air temperature. A Roots blower was connected to the exhaust pipe for the tests with reduced back pressure. The standard test-engine equipment was used for measuring brake mean effective pressure, engine speed, fuel consumption, and air temperature at the inlet to the carburetor.

METHODS AND TESTS

Calibration tests were made to determine the weight of air flowing over the head and the barrel as functions of the pressure drop across the cylinder. The calibration curves are shown in figure 3.

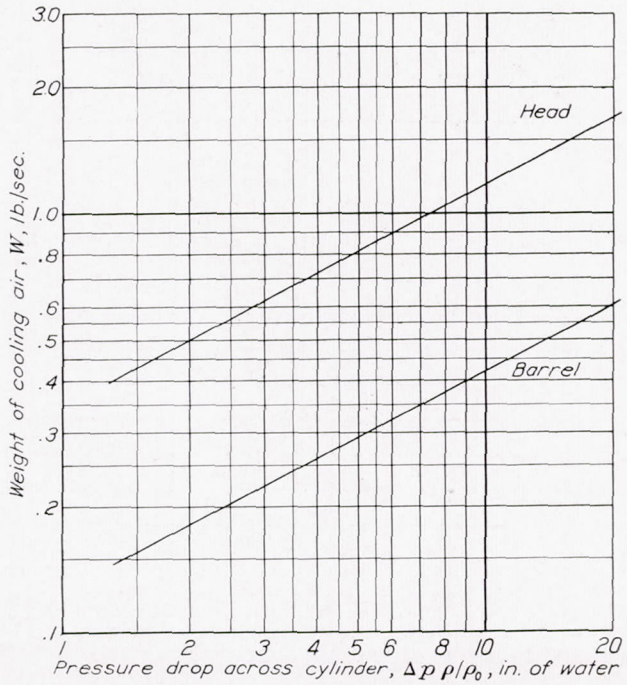

FIGURE 3.—Calibration of the jacket as an air duct. Slope, 0.53.

Tests were conducted in which each of the following factors was varied in turn while the remaining factors were held constant:

1. Cooling-air temperature.
2. Brake mean effective pressure.
3. Engine speed.
4. Mass flow of cooling air.
5. Fuel-air ratio.
6. Spark setting.
7. Carburetor-air temperature.
8. Exhaust pressure.

In all of the tests with the exception of the ones in which the brake mean effective pressure was varied, the weight of the charge delivered to the engine per cycle was held constant.

The tests covered the following ranges of conditions:

Cooling-air temperature, °F	80–225.
Brake mean effective pressure, pounds per square inch	65–154.
Engine speed, r. p. m	1,300–2,000.
Pressure drop across cylinder, inches of water	2.2–13.2.
Fuel-air ratio	0.058–0.098.
Spark setting, degrees B. T. C	10–25.
Carburetor-air temperature, °F	82–284.
Exhaust pressure, inches of mercury absolute	12.1–29.5.

The validity of the analysis over a range of engine and cooling conditions was checked by making more tests than were necessary to establish the values of the constants in the equations. The methods of conducting the tests and calculating and plotting the data are fully described in reference 1.

The friction horsepower was determined by motoring the engine at the manifold pressures, the exhaust pressures, and the speeds used in the power runs. The indicated horsepower was obtained by adding the gross brake to the friction horsepower.

In the tests with reduced exhaust back pressure to obtain the indicated horsepowers, the friction horsepowers should correspond to operation with these reduced pressures. These friction horsepowers were estimated by deducting from the friction as obtained at atmospheric back pressure the change in work done by the piston in exhausting the cylinder on the assumption that, for the greater part of the piston motion, the difference in pressure in the cylinder is equal to the difference in back pressure. The following expression was used to determine the corrected indicated horsepower:

$$I_{corr} = I_{scale} - I_{ex}$$

where

$$I_{ex} = \frac{\Delta p_1 L A_c N}{33{,}000 \times 2}$$

$$\Delta p_1 = \frac{29.92 - \text{absolute exhaust pressure}}{29.92} 14.7,$$

pounds per square inch.

L, stroke, feet.

A_c, cross-sectional area of piston, square inches.

N, engine speed, revolutions per minute.

The weight of gases in the cylinder W_t was obtained by adding the weight of air, fuel, and residuals. The weight of air was obtained by dividing the weight of fuel by the fuel-air ratio. The weight of residuals was considered to be the weight of air in the clearance volume at an absolute temperature of 1,660° F. and a pressure equal to the exhaust pressure.

Gasoline conforming to U. S. Army specification Y–3557 and having an octane number of 87 was used for most of the tests. For the more severe operating conditions, a sufficient amount of ethyl fluid was added to the fuel to suppress audible knock.

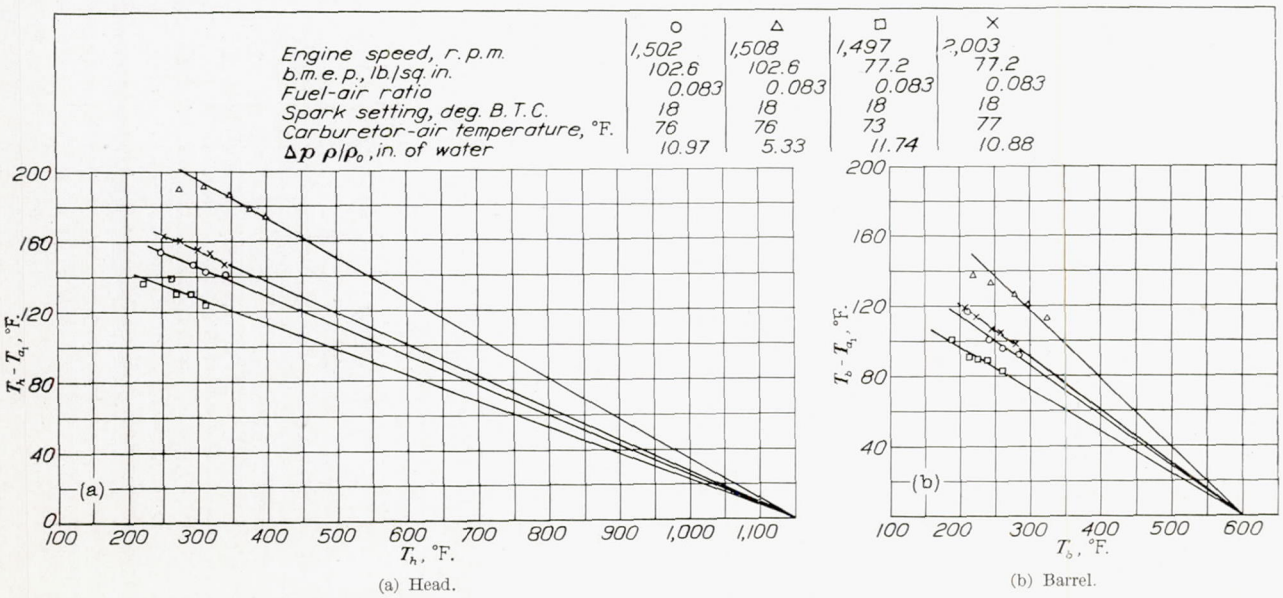

(a) Head. (b) Barrel.

FIGURE 4.—Variation of $T_h - T_{a_1}$ and $T_b - T_{a_1}$ with head and barrel temperatures.

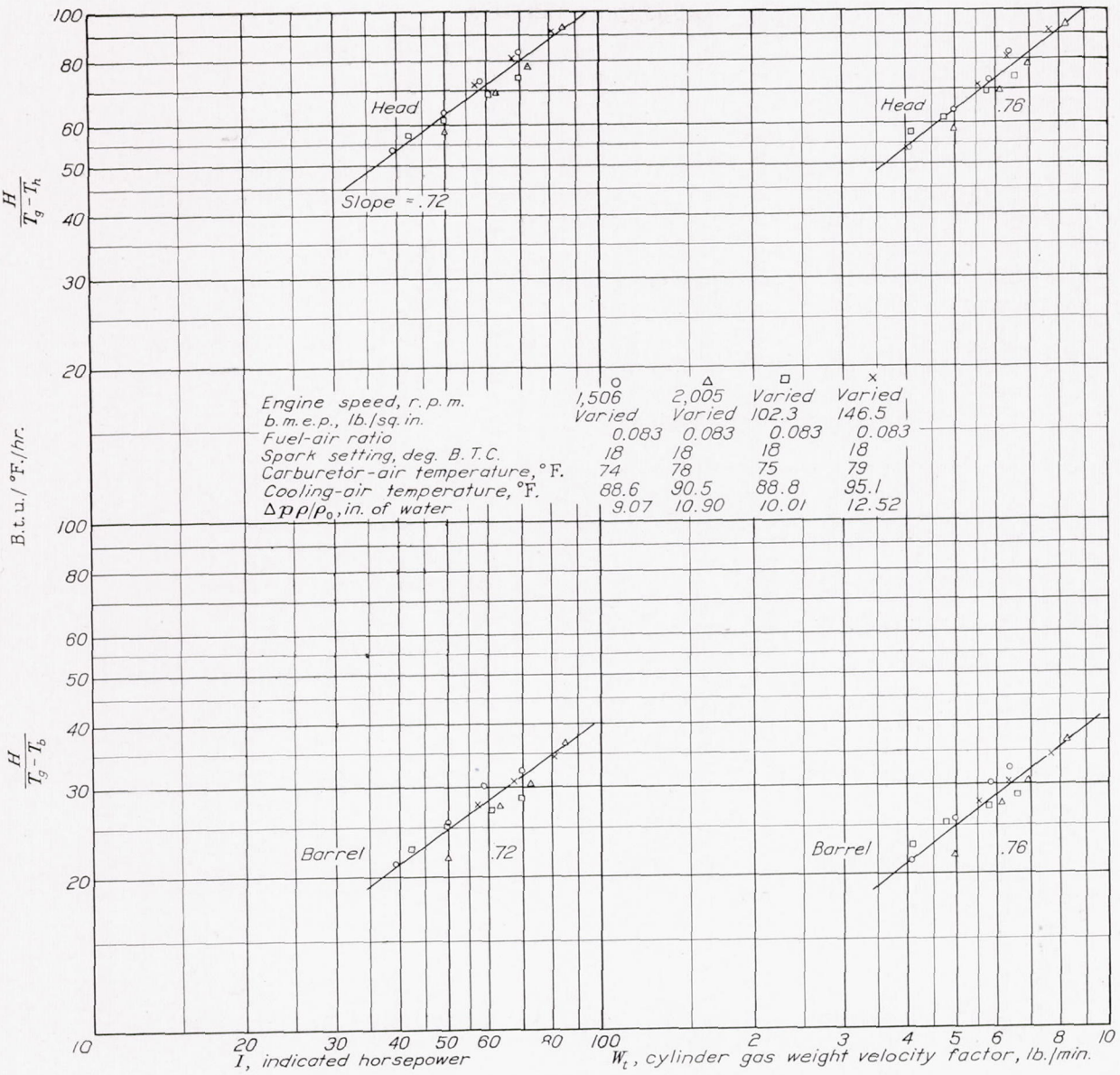

FIGURE 5.—Variation of $H/(T_g-T_h)$ and $H/(T_g-T_b)$ with I and W_t.

RESULTS AND DISCUSSION

AVERAGE CYLINDER TEMPERATURE

Gas temperature.—It has been shown in reference 1 that the effective gas temperature T_g may be obtained by plotting curves of temperature difference between the cylinder and the cooling air against cylinder temperature from tests in which all of the conditions except the cooling-air temperature are maintained constant. The value of T_g is found by extrapolating such curves to the axis $T_h - T_{a_1} = 0$.

Figure 4 shows four sets of data, which were obtained in the present tests, for determining T_g for the 1820–G cylinder. The accuracy of the equations for determining the cylinder head and barrel temperatures is not very sensitive to the initial value of T_g. Once a value of T_g has been chosen, it is much more important that the variation of T_g from the initial value with change in fuel-air ratio, carburetor-air temperature, and spark timing be accurate. Consideration of a large amount of data (references 1 and 2) has led to a choice of values of T_g of 1,150° F. for the cylinder head and 600° F. for the cylinder barrel at a fuel-air ratio of 0.08, a carburetor-air temperature of 80° F., and normal spark timing. Although slight variations from these values of T_g occur for the cylinders tested, the foregoing values were chosen as standards to simplify the comparison of engines with little sacrifice in the accuracy of the equations. The values of 1,150° F. and 600° F. are seen to fit the data plotted in figure 4 as well as any other pairs of values that could be chosen. The effective gas temperature T_g is a means of correlating engine-cooling data; it cannot be used as an accurate measure of combustion-gas temperature.

194665—40——2

Heat transfer from combustion gas to cylinder.—The values of $H/(T_g-T_h)$ and $H/(T_g-T_b)$ were calculated from test data obtained at various engine speeds and manifold pressures for a fuel-air ratio of 0.083. The results are plotted against I and W_t (see equations (2) and (1)) on logarithmic coordinates in figure 5. The points fall on the same curve whether the indicated horsepower was varied by varying the engine speed or the manifold pressure, as was found in reference 1, which indicates that the analysis is sufficiently close for the present range of speeds. The exponents in equations (1) and (2) as obtained from the slope of the curves in figure 5 are $n=0.76$ and $n'=0.72$ for both the head and the barrel.

The exponents n and n' may also be obtained by plotting $(T_h-T_{a_1})/(T_g-T_h)$ and $(T_b-T_{a_1})/(T_g-T_b)$ against I and W_t for tests in which $\Delta p\rho/\rho_0$ was held constant. (See equation (9).) These curves are shown in figure 6, and it is seen that lines with the same slopes as those in figure 5 represent the data very well.

The constants for equations (1) and (2) were obtained from figure 5; the equations are tabulated as follows:

Head	Barrel
$H=3.75\ I^{0.72}(T_g-T_h)$	$H=1.48\ I^{0.72}(T_g-T_b)$
$H=18.72\ W_t^{0.76}(T_g-T_h)$	$H=7.33\ W_t^{0.76}(T_g-T_b)$

(31)

Units of H are B. t. u. per hour; units of W_t are pounds per minute.

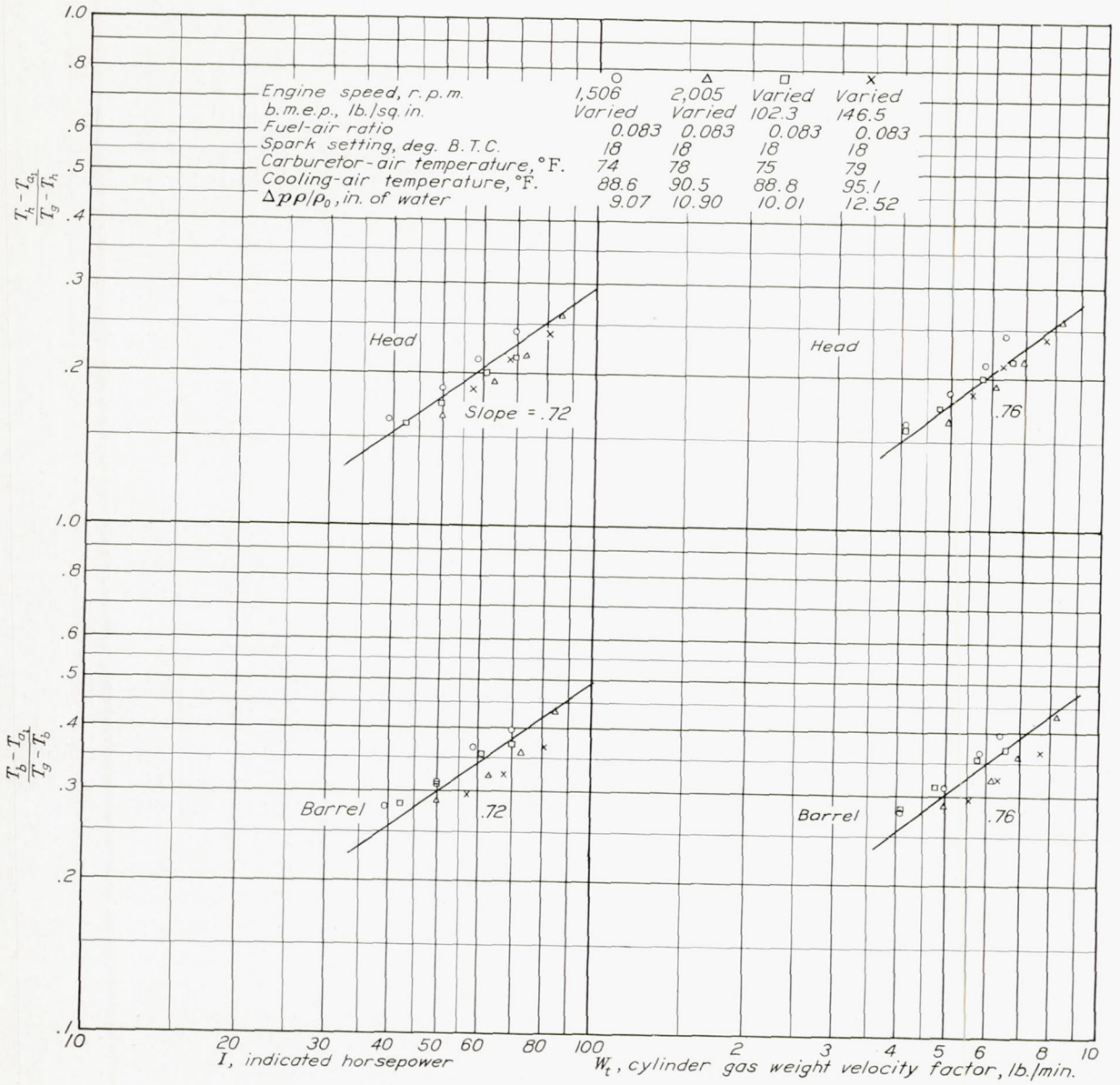

FIGURE 6.—Variation of $(T_h-T_{a_1})/(T_g-T_h)$ and $(T_b-T_{a_1})/(T_g-T_b)$ with I and W_t.

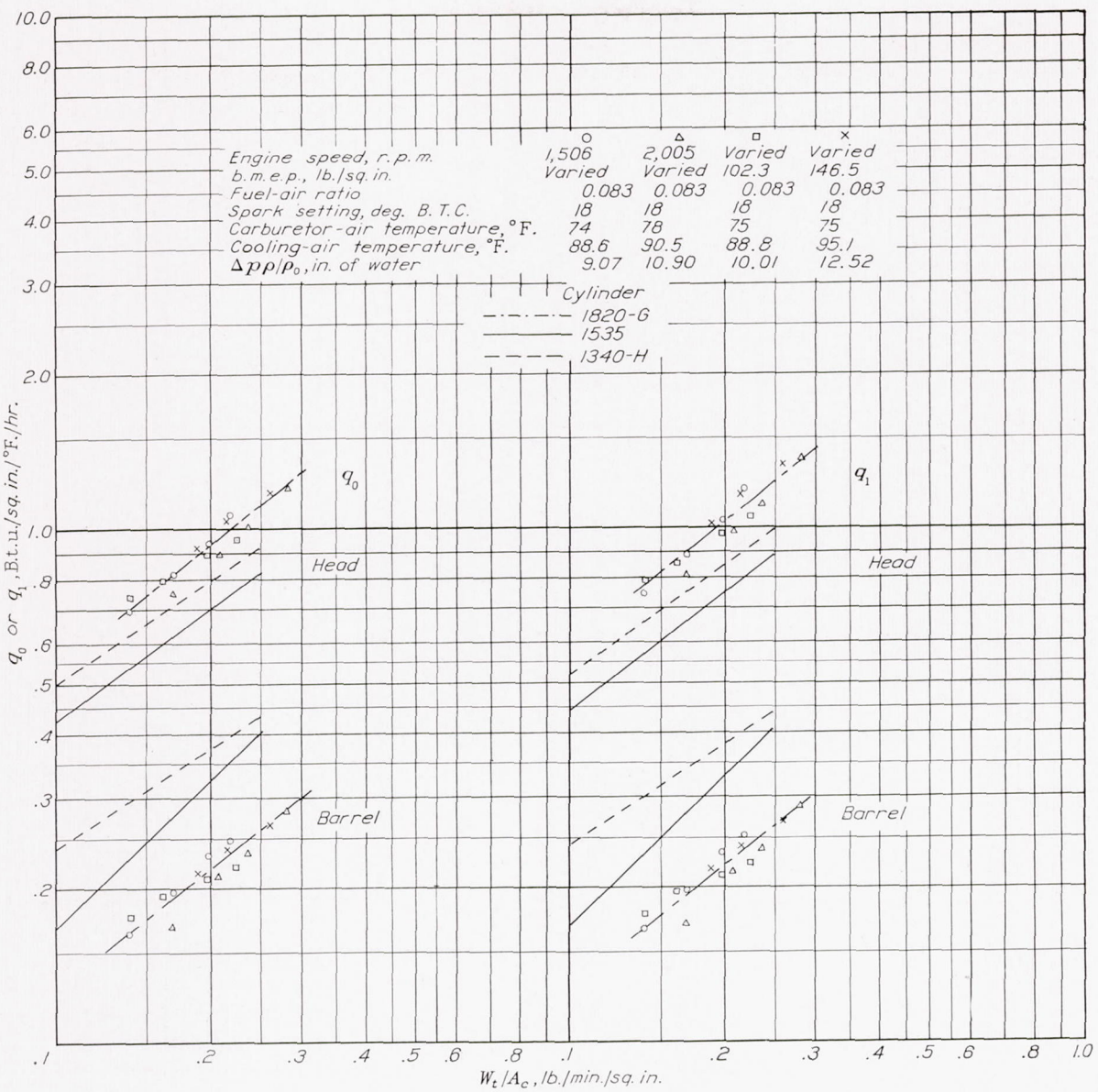

FIGURE 7.—Variation of heat-transfer coefficient from combustion gases to head and barrel with W_t/A_c.

The heat-transfer coefficients from the combustion gas to the cylinder wall for the three cylinders are shown in figure 7. The data for the 1535 and the 1340–H cylinders were obtained from reference 1. The coefficients are plotted against the ratio W_t/A_c, which is used as a criterion of the mass flow of the gas in the cylinder. Little difference in the coefficients for the barrel of any one cylinder is obtained, whether they are based on the difference in temperature between the gas and the inside wall or on the difference in temperature between the gas and the outside wall. This small difference in the coefficients is due to the fact that the barrel wall is thin and the temperature drop through it is negligible. For the head, however, q_1 is approximately 7 percent higher than q_0 for all the cylinders.

Variation of T_g with engine conditions.—The values of T_g for the tests in which fuel-air ratio, spark setting, carburetor-air temperature, and exhaust pressure were varied were calculated from the test results using equations (31). Two curves were obtained for the head and the barrel by using, in turn, the equations involving I and W_t. Figure 8 shows the values of T_g plotted against fuel-air ratio. The value of T_g is seen to be substantially independent of engine speed and brake mean effective pressure. A greater range of fuel-air ratio was covered in the present tests than in previous tests. As the fuel-air ratio is decreased below the value for the theoretically correct mixture, T_g decreases. Thus, lower cylinder temperatures will result from operation with either rich or lean mixtures than with the theoretically correct mixture.

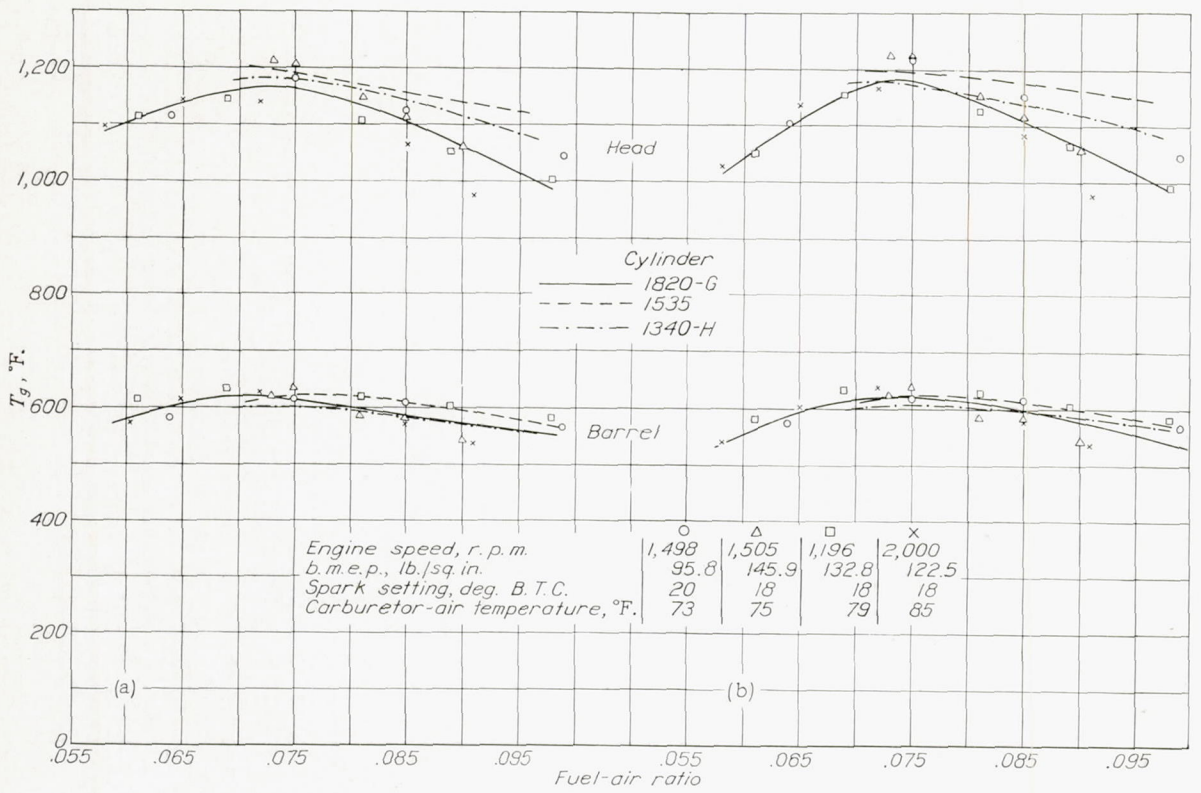

(a) T_g based on indicated horsepower, I. (b) T_g based on cylinder gas weight flow factor W_t.

FIGURE 8.—Variation of T_g with fuel-air ratio.

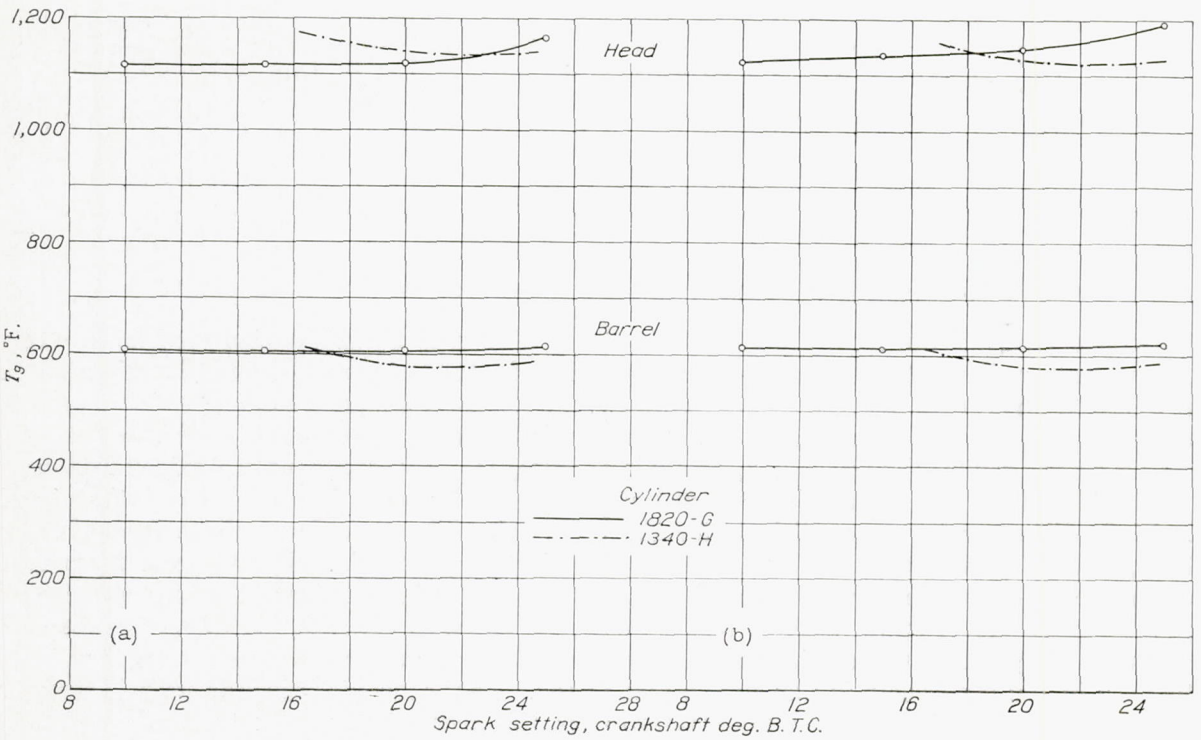

(a) T_g based on indicated horsepower, I. (b) T_g based on cylinder gas weight flow factor, W_t.

FIGURE 9.—Variation of T_g with spark setting. Test points indicate data obtained under the following conditions: Fuel-air ratio, 0.083; carburetor-air temperature, 74° F; engine speed, 1,502 r. p. m.; brake mean effective pressure, 102.2 pounds per square inch.

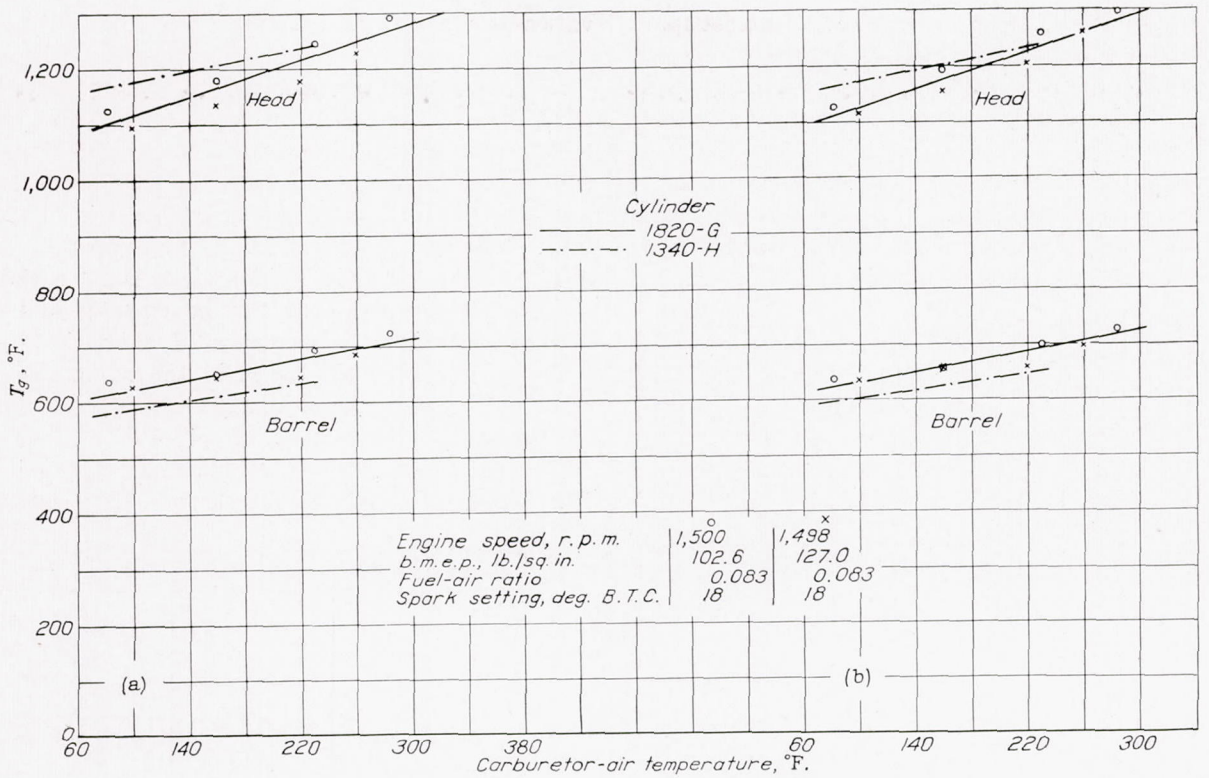

(a) T_g based on indicated horsepower, I. (b) T_g based on cylinder gas weight flow factor, W_f.

FIGURE 10.—Variation of T_g with carburetor-air temperature.

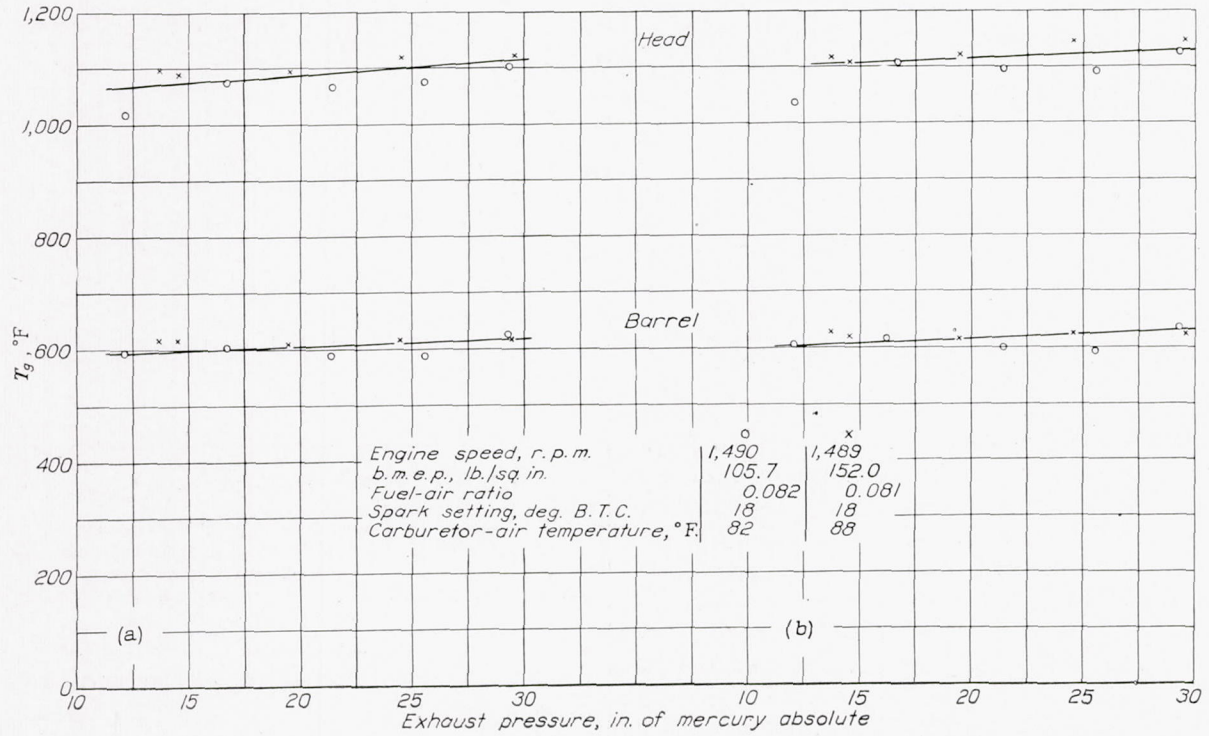

(a) T_g based on indicated horsepower, I. (b) T_g based on cylinder gas weight flow factor, W_f.

FIGURE 11.—Variation of T_g with exhaust pressure.

194665—40——3

Figure 9 shows the values of T_g plotted against spark setting. The value of T_g remains essentially constant over a range of spark settings covering usual operating conditions; it increases, however, for greatly advanced spark settings.

The results of the tests to determine the effect of carburetor-air temperature on T_g are shown in figure 10. As was previously determined, T_g increases appreciably as the carburetor-air temperature increases. An increase in T_g of 0.8° F. per degree rise in carburetor-air temperature is noted for the head. Curves (reproduced from reference 1) representing the values of T_g for the 1535 cylinder at various fuel-air ratios are shown in figure 8 and, for the 1340–H cylinder at various fuel-air ratios, spark settings, and carburetor-air temperatures, are included in figures 8, 9, and 10 for comparison with the results for the 1820–G cylinder.

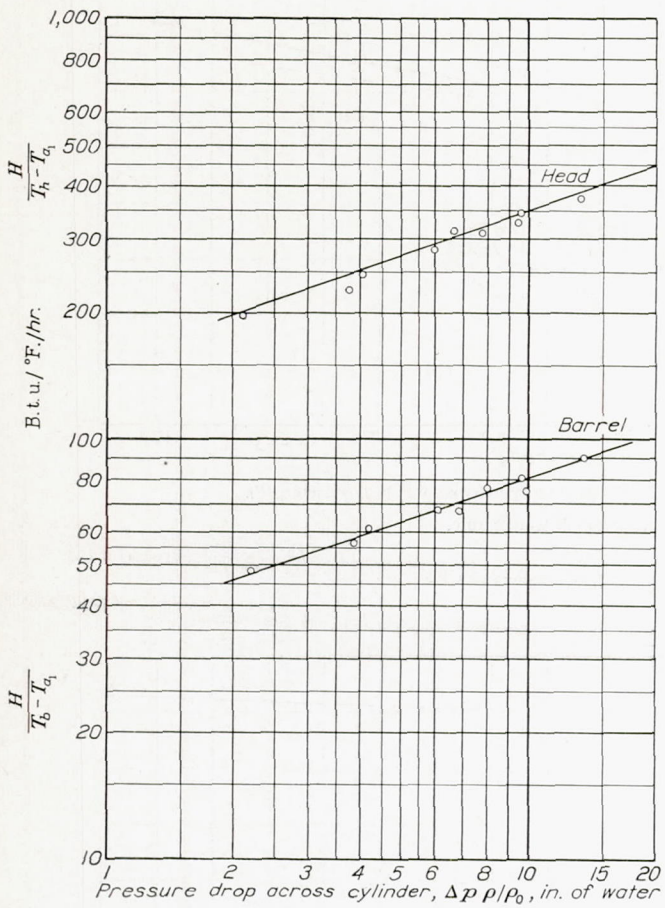

FIGURE 12.—Variation of $H/(T_h - T_{a_1})$ and $H/(T_b - T_{a_1})$ with pressure drop across cylinder. Slope, 0.35; fuel-air ratio, 0.085; cooling-air temperature, 87.0° F.; carburetor-air temperature, 82° F.; engine speed, 1,503 r. p. m.; brake mean effective pressure, 102.5 pounds per square inch; spark setting, 20° B. T. C.

The effective gas temperature T_g over the range tested varied little as the exhaust pressure was varied, as shown in figure 11. The curve based on indicated horsepower in figure 11 was calculated from the indicated horsepower corrected as previously explained. The results of the tests shown in figure 11 bear out the assumption made in reference 1 that the weight of residuals, which varies as the exhaust pressure varies, has only a small effect on T_g.

Heat transfer from cylinder to cooling air.—Values of $H/(T_h - T_{a_1})$ and $H/(T_b - T_{a_1})$ are plotted in figure 12 on logarithmic coordinates against $\Delta p\rho/\rho_0$. The exponent m in equation (3) for both the head and the barrel as obtained from the slopes of the lines in figure 12 is 0.35. The exact agreement of the exponents for the head and the barrel is accidental, as some variation in the value of the exponent may be expected with difference in fin design. For constant I, the ratio $(T_g - T_h)/(T_h - T_{a_1})$ varies with $\Delta p\rho/\rho_0$ in the same manner as $H/(T_h - T_{a_1})$. (See equations (9) and (3).) As a check on figure 12, the values of $(T_g - T_h)/(T_h - T_{a_1})$ and $(T_g - T_b)/(T_b - T_{a_1})$ were plotted against $\Delta p\rho/\rho_0$ in figure 13. Values of 1,150° F. and 600° F. were used for T_g for the head and the barrel, respectively. The exponents m obtained from figure 13 check those obtained from figure 12.

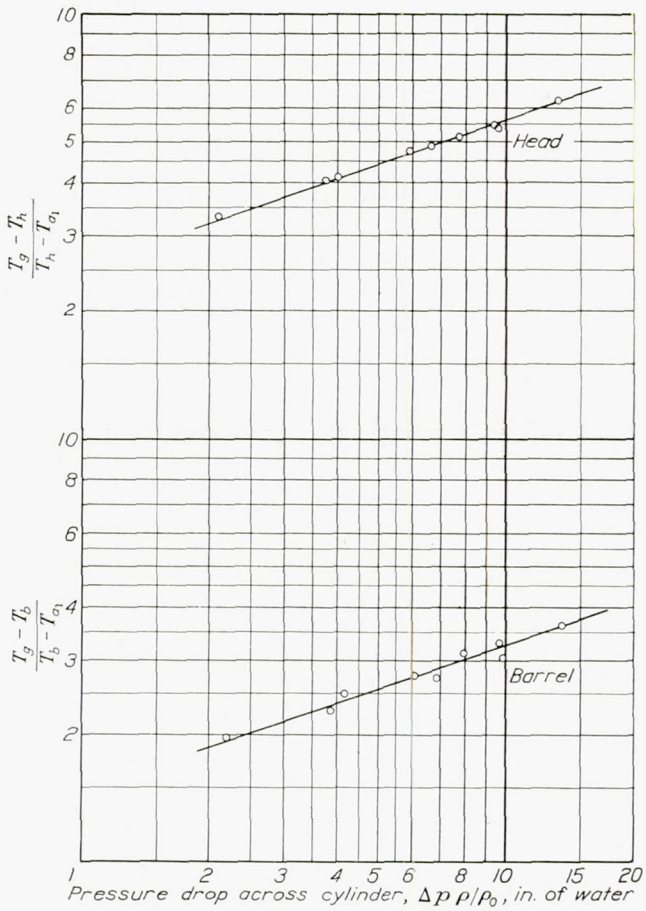

FIGURE 13.—Variation of $(T_g - T_h)/(T_h - T_{a_1})$ and $(T_g - T_b)/(T_b - T_{a_1})$ with pressure drop across cylinder. Slope, 0.35; fuel-air ratio, 0.085; cooling-air temperature, 87.0° F.; carburetor-air temperature, 82° F.; engine speed, 1,503 r. p. m.; brake mean effective pressure, 102.5 pounds per square inch; spark setting, 20° B. T. C.

The constants for equation (3) were obtained from figure 12 and are:

$$\left.\begin{aligned} \text{Head: } H &= 154\ (\Delta p\rho/\rho_0)^{0.35}\ (T_h - T_{a_1}) \\ \text{Barrel: } H &= 36.3\ (\Delta p\rho/\rho_0)^{0.35}\ (T_b - T_{a_1}) \end{aligned}\right\} \quad (32)$$

Units of H are B. t. u. per hour; units of Δp are inches of water.

Average head and barrel temperatures.—If H is eliminated between equations (31) and (32), expressions may be obtained for T_h and T_b in the form given by equation (4). Thus, for the 1820–G cylinder, the average head and barrel temperatures may be expressed as functions of the indicated horsepower and pressure drop as follows:

$$\left.\begin{aligned} T_h - T_{a_1} &= \frac{T_g - T_{a_1}}{\frac{154\,(\Delta p \rho/\rho_0)^{0.35}}{3.75\,I^{0.72}} + 1} \\ T_b - T_{a_1} &= \frac{T_g - T_{a_1}}{\frac{36.3\,(\Delta p \rho/\rho_0)^{0.35}}{1.48\,I^{0.72}} + 1} \end{aligned}\right\} \qquad (33)$$

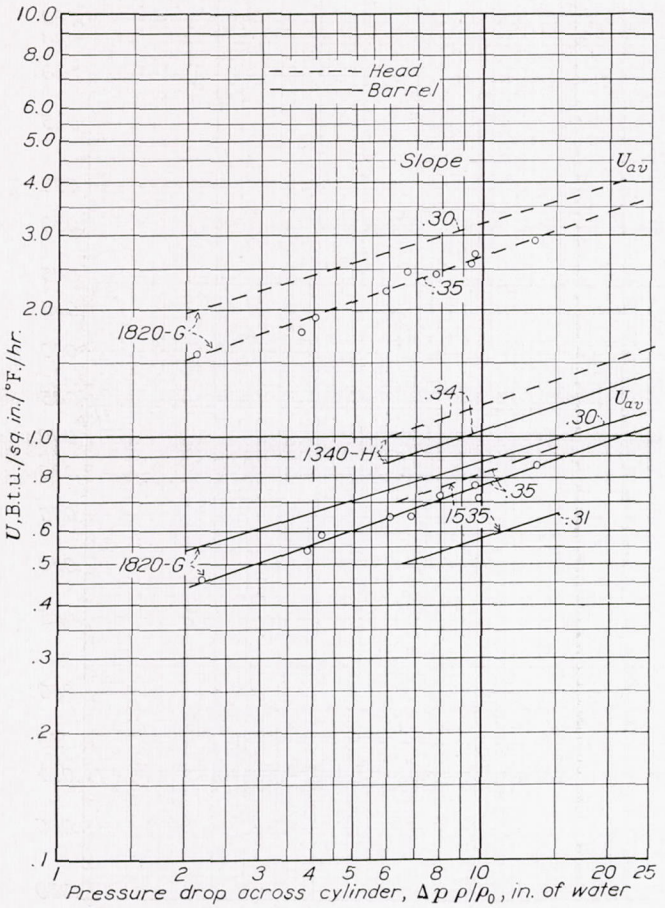

FIGURE 14.—Variation of heat-transfer coefficient from head and barrel to cooling air with pressure drop across cylinder. Test points indicate data obtained under the following conditions: Fuel-air ratio, 0.085; cooling-air temperature, 87.0° F.; carburetor-air temperature, 82° F.; engine speed, 1,505 r. p. m.; brake mean effective pressure, 102.5 pounds per square inch; spark setting, 20° B. T. C.

Equations similar to (33) will apply to flight conditions with the exception that the constant before the pressure drop may be greater.

Figure 14 shows the heat-transfer coefficients U from the cylinder to the cooling air plotted against the pressure difference for the heads and the barrels of the three cylinders. The coefficients for the head of the 1820–G cylinder are much greater than those of the other cylinders on account of its better finning. Any of the curves in figure 14 would probably be raised if some device to create turbulence were placed in front of the cylinders. The turbulence condition would be a closer approach to flight conditions.

Figure 15 shows the wall heat-transfer coefficients of electrically heated cylinders with fin designs as on the heads and barrels of the 1820–G, the 1340–H, and

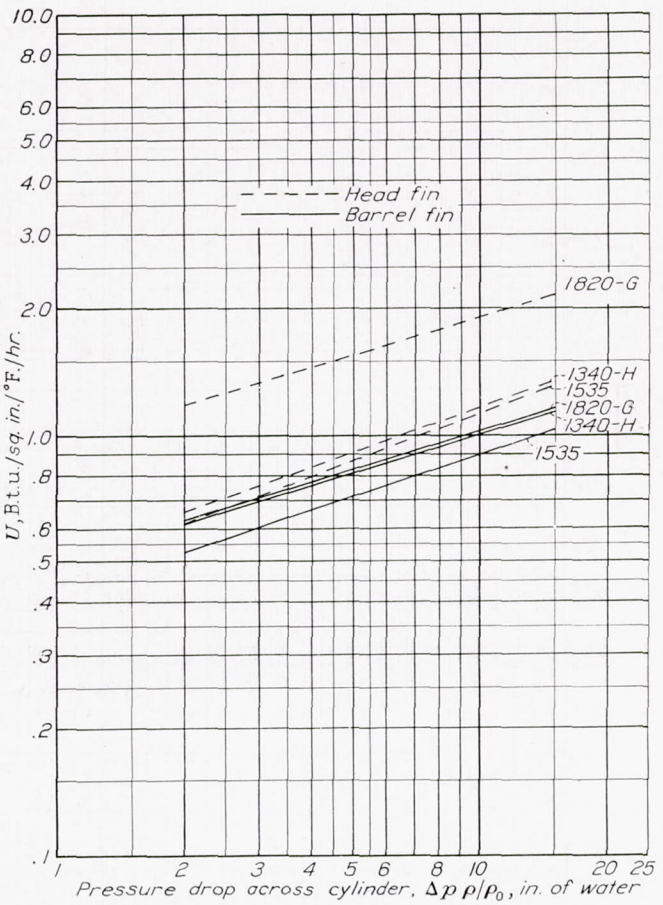

FIGURE 15.—Variation of heat-transfer coefficient from cylinder wall to cooling air of electrically heated cylinders with pressure drop across cylinder.

the 1535 cylinders, calculated from data on the surface heat-transfer coefficients for cylinders enclosed in jackets and cooled by a blower (reference 3). Although the jacket and the flow conditions are different for the electrically heated and the engine cylinders, figure 15 again shows that the 1820–G head fins give much higher coefficients than those of the other cylinders. The areas for the various cylinders are listed in the following table:

TABLE I

Cylinder	a_1 (sq. in.)		a_0 (sq. in.)		A_c (sq. in.)
	Head	*Barrel*	*Head*	*Barrel*	
1535	47.1	82.6	94.5	61.5	21.1
1340–H	76.8	84.2	142.0	68.5	25.9
1820–G	77.7	130.0	127.1	104.7	29.5

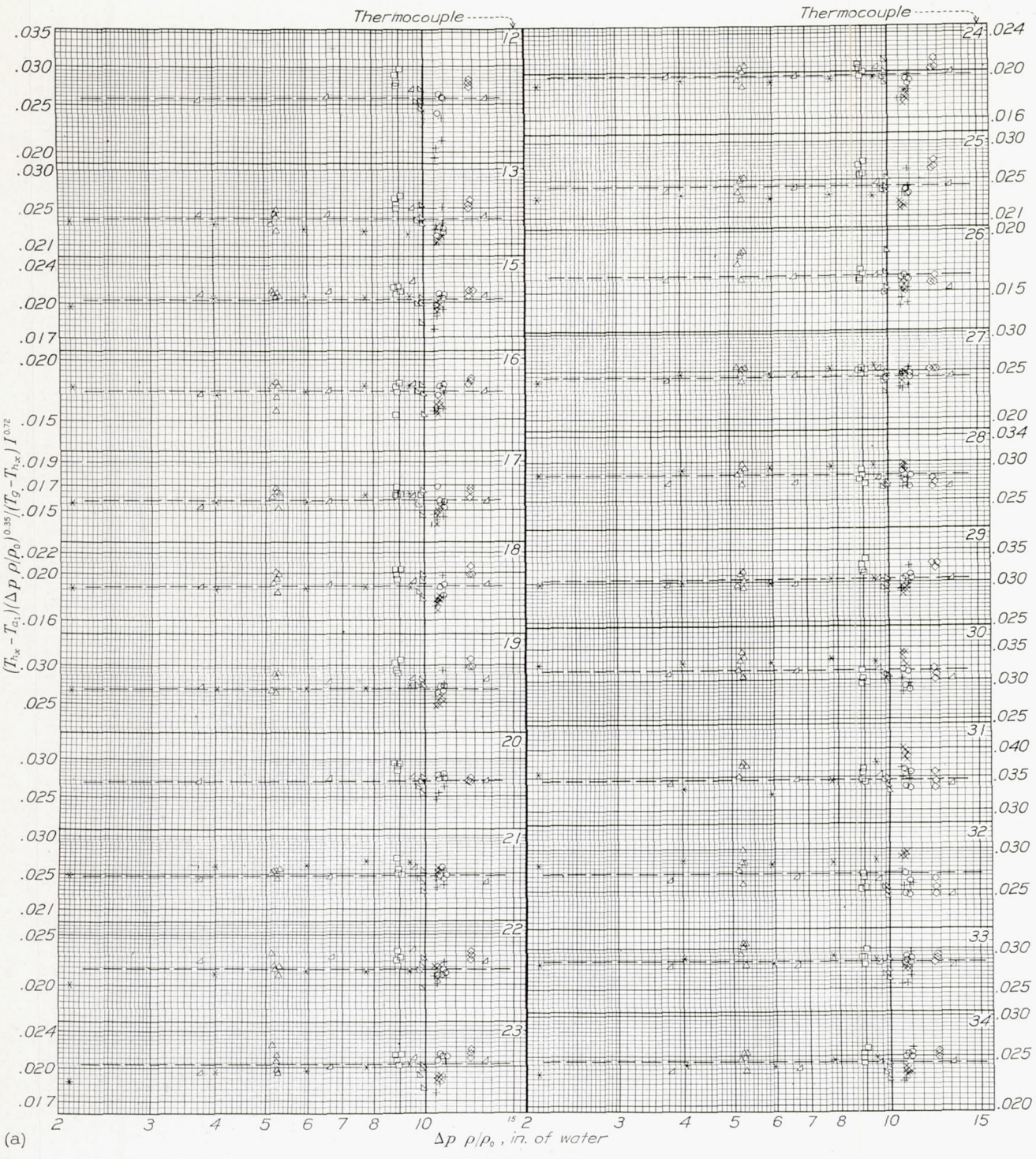

(a) Head temperatures.

FIGURE 16.—Correlation of temperatures at several locations with engine and cooling conditions.

TEMPERATURE AT INDIVIDUAL POINTS ON CYLINDER

The following relation holds for the temperatures at individual points on the cylinder with T_g replaced by T_{g_x}. (See equation (30).)

$$\frac{(\Delta p\rho/\rho_0)^m}{I^{n'}}\ \frac{T_{h_x}-T_{a_1}}{T_{g_x}-T_{h_x}}=f_2(\Delta p\rho/\rho_0)$$

As discussed in the appendix, some variation probably exists in the effective gas temperature T_{g_x} for individual locations on the cylinder. In the absence of data on this effect, the values of T_{g_x} for all points on the head were arbitrarily taken equal to T_g and the same was done for the barrel. The validity of this assumption may be checked to some extent by the closeness with

which the points obtained by plotting the left-hand side of equation (30) against $\Delta p\rho/\rho_0$ fall on a single curve for all test conditions.

Figure 16 shows such a plot for the various points on the head and the barrel. Some scatter of the points from a single curve is noted. No trend with any of the variables could be observed. The points are too far apart to permit a conclusion to be drawn with regard to the assumption of $T_{g_x}=T_g$; the curves indicate, however, that the use of $T_{g_x}=T_g$ gives a correlation of the test data for individual points sufficiently close for practical purposes. For all the cases shown in figure 16, the slope of the curve is small and, for most of the thermocouple locations, $f_2(\Delta p\rho/\rho_0)$ in equation (30) can be replaced by a constant. Equations of the form of (10a) and (10b) with T_h replaced by T_{h_x} may then be used for correlating these data.

APPLICATIONS

Comparison of cooling of cylinders.—Cooling tests of a 1340–H cylinder have been conducted in the laboratory on a single-cylinder test engine (reference 1).

	○	□	×	+	△	◺	◇	⏢	*
Engine speed, r.p.m.	1,502	1,506	2,003	2,005	1,508	Varied	Varied	1,503	1,504
b.m.e.p., lb./sq. in.	102.6	Varied	77.2	Varied	102.6	102.3	146.5	102.5	102.3
Indicated horsepower	49.8	Varied	55.5	Varied	49.9	Varied	Varied	49.7	48.8
Spark setting, deg. B. T. C.	18	18	18	18	18	18	18	20	18
Carburetor-air temperature, °F.	76	74	77	78	76	75	79	75	88
Air-fuel ratio	12.0	12.0	12.0	12.0	12.0	12.0	12.0	12.0	11.6
Cooling-air temperature, °F.	Varied	88.6	Varied	90.5	Varied	88.8	95.1	87.0	87.2
$\Delta p\ \rho/\rho_0$, in. of water	10.97	9.07	10.88	10.90	5.33	10.01	12.52	Varied	Varied

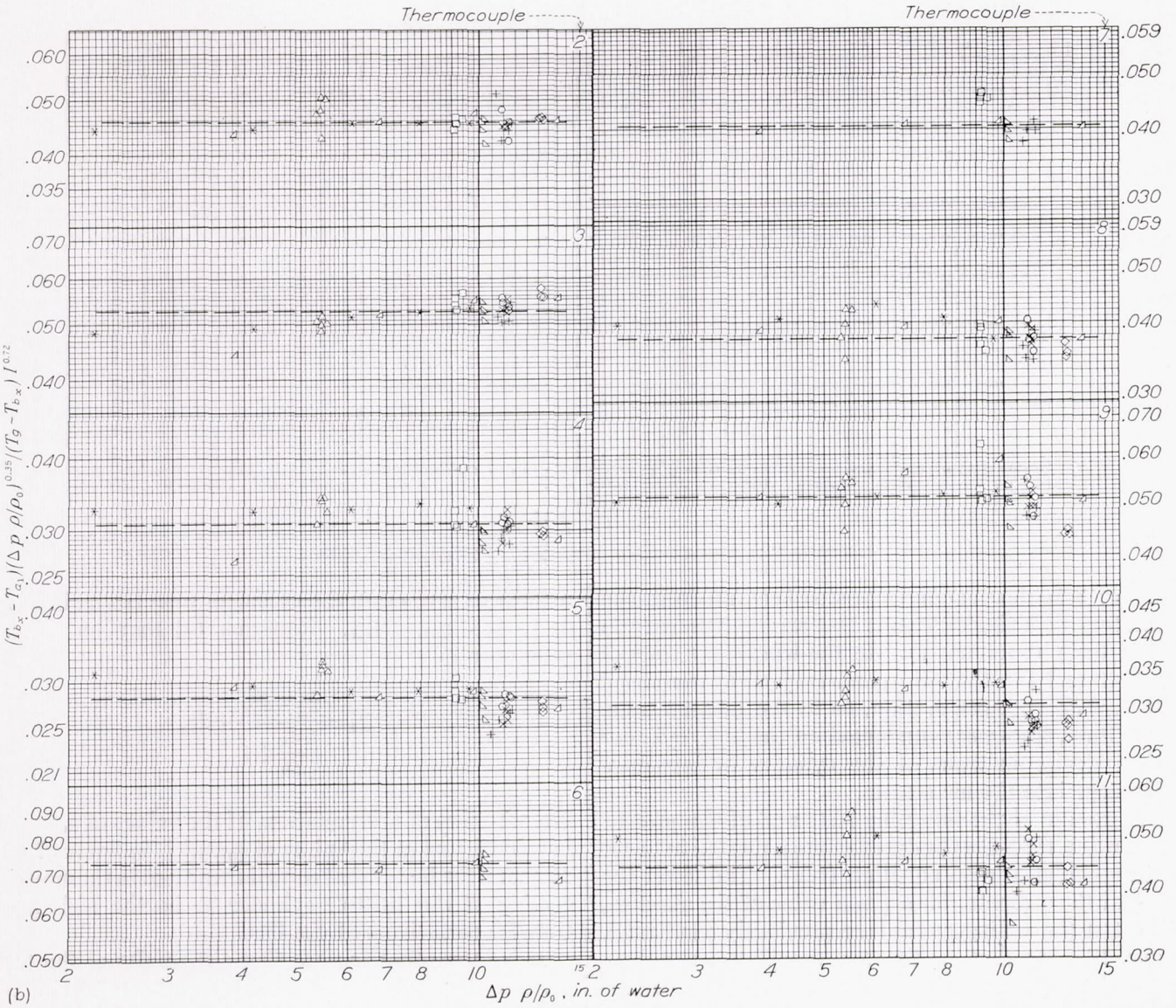

(b) Barrel temperatures.

FIGURE 16.—Continued. Correlation of temperatures at several locations with engine and cooling conditions.

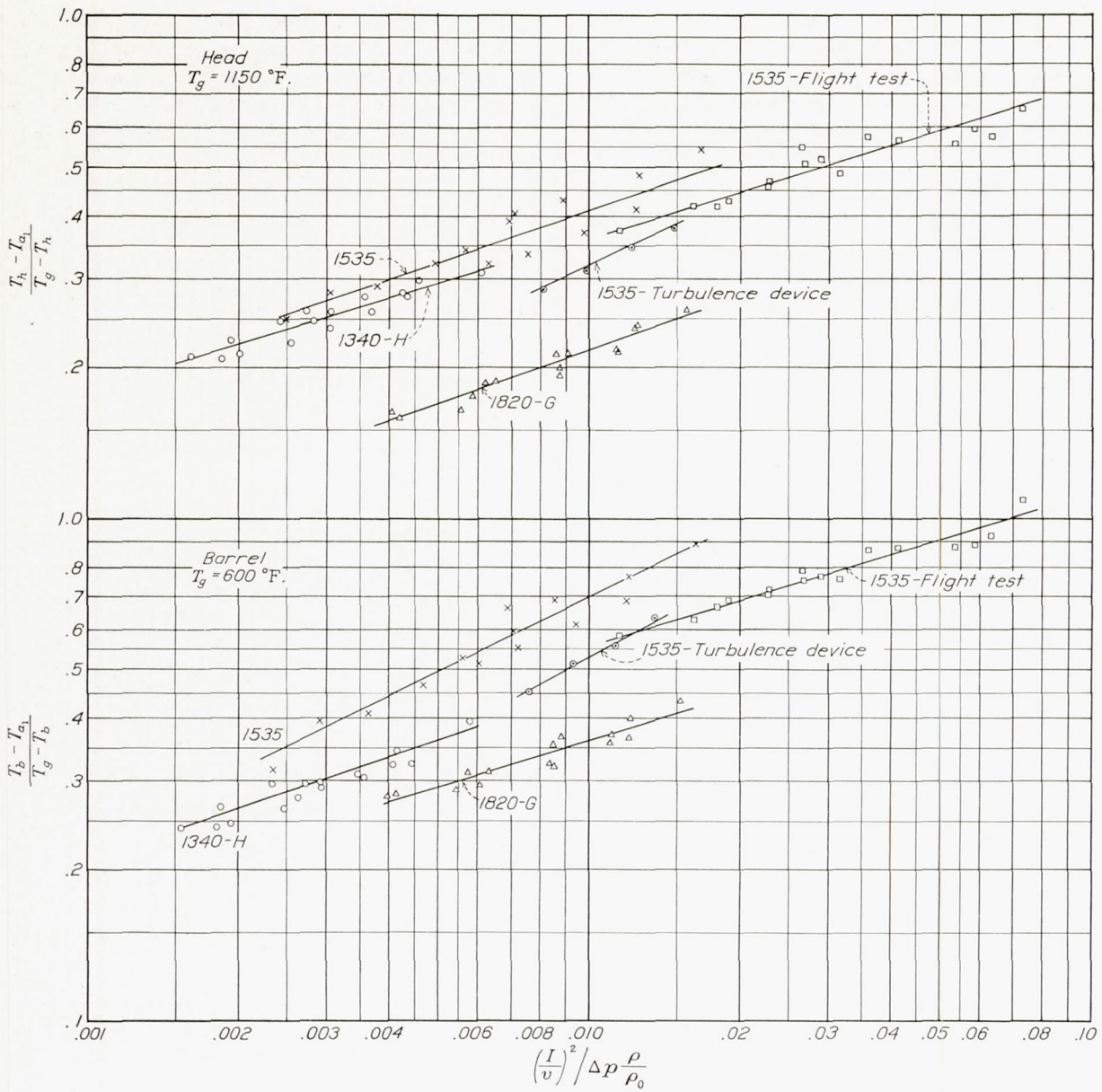

FIGURE 17.—Comparison of cooling of several cylinders in laboratory and in flight.

Tests of a 1535 cylinder have also been made in the laboratory on a single-cylinder test engine (reference 1) and in flight (reference 4). In the laboratory tests of the 1535 and the 1340–H cylinders, jackets were used with a wide entrance section, as in the present tests. In addition, tests were conducted on the 1535 cylinder with a device in front of the cylinder to introduce turbulence into the air stream.

The results of the foregoing tests and of the present tests on the 1820–G cylinder are shown plotted in figure 17 in accordance with equation (10a). The lower the value of the ordinate, for a given value of the abscissa, the better the cooling, as has been previously mentioned. Figure 17 shows that, for the same specific power output and cooling pressure drop, the temperatures of the 1820–G cylinder are lower than those of the 1535 and the 1340–H cylinders for both the head and the barrel, regardless of whether the cylinders were tested in flight or in the laboratory. Equation (4) may be written (reference 1)

$$T_h = \frac{T_g - T_{a_1}}{\frac{U a_0}{q_0 a_1} + 1} + T_{a_1}$$

Examination of this equation, of the values of a_0 and a_1 in table I, and of the values of q_0 and U in figures 7 and 14 shows the factor that contributes most to the superior cooling of the 1820–G cylinder to be the high heat-transfer coefficients of the fins.

It is interesting to note that the results of the tests on the 1535 cylinder with the turbulence device are very nearly the same as those for the flight tests on the same cylinder.

Figure 17 shows that the assumption $n'/m=2$, made in obtaining equation (10a), does not cause the data to scatter to any appreciable extent. This approximation was introduced to simplify the comparison of the cooling data of different engines. If considerable difference exists between n'/m and 2 for a given engine, then a series of closely grouped curves will be obtained when the data are plotted as in figure 17, in which each curve will be identified by a given value of $\Delta p\rho/\rho_0$. The relation of this group to the curve or group of curves for other engines will indicate the comparative cooling. The data obtained for any given engine can, of course, be plotted as a single curve when the values of n' and m for that engine are used in obtaining n'/m.

Figure 18 presents another illustration of the same application. The data were obtained from Navy reports on routine calibration tests of a number of service engines. The operating ranges covered by the points in figure 18 are listed in the following table.

Engine	Engine speed (r. p. m.)	Engine b. m. e. p. (lb./sq.in.)	Cooling-air velocity in duct (m. p. h.)	Fuel-air ratio	Altitude (ft.)
Wright R–2600	1, 700–2, 300	82–171	225	0. 077–0. 092	9, 500–18, 000
Wright R–1820–G	1, 105–2, 100	86–176	140–210	. 062– . 097	0
Pratt & Whitney R–1535	1, 610–2, 420	106–160	200	. 058– . 085	0– 5, 100
Pratt & Whitney R–1340–D	1, 490–2, 425	80–148	173	. 058– . 085	0

The values of T_{h_x} represent an average of the maximum and minimum temperatures of the rear spark-plug gasket for each test condition. Inasmuch as the velocity of the cooling air rather than the pressure drop across the engine was measured, an equation similar to (10b) was used in plotting figure 18. The value of T_g for the various fuel-air ratios was taken from figure 8 for the Wright R–1820–G and R–2600 engines and from reference 1 for the Pratt & Whitney R–1340–D and R–1535 engines. The fact that a single curve for each engine is obtained in figure 18 for all the engine and cooling conditions further supports the use of T_g for the value of T_{g_x} in the neighborhood of the rear spark plug. Good correlation, however, can be obtained with somewhat higher or lower values of T_{g_x} and the results in figure 18 cannot be taken as proof that the value of T_{g_x} is exactly that of T_g. The Wright R–2600 and R–1820–G engines both use the same type of cylinder, and a single curve for both engines in figure 18 would be expected.

The lower the curve in figure 18 the better the cooling, as indicated by the rear spark-plug temperature. To base a comparison of the cooling of two different engines on the rear spark-plug temperatures, as is usually done, is not entirely correct. The rear spark-plug temperatures and the temperatures at other hot spots are important when difficulty is experienced with preignition and spark-plug failure. The tendency of an engine to detonate depends, among other things, on the temperature of the engine charge, which depends more on the average head and barrel temperature than on the temperature at localized hot spots. The average head and barrel temperatures rather than rear spark-plug temperatures also control lubricating-oil temperatures. Thus, when no difficulty is experienced with preignition or spark-plug failure, the average head and barrel temperatures are more important criterions of cooling than the rear spark-plug temperatures. For example, it is permissible to operate a Pratt & Whitney R–1535

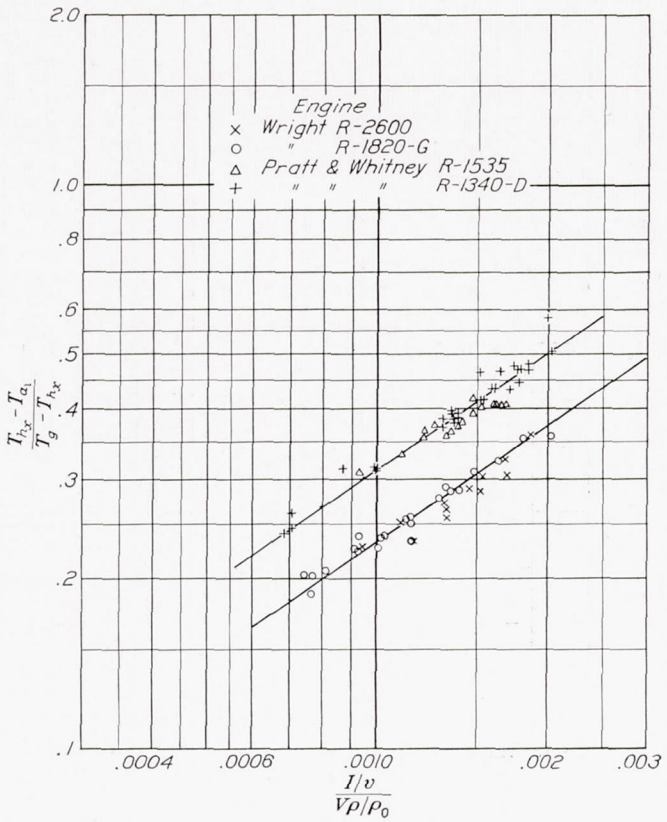

FIGURE 18.—Variation of spark-plug-boss temperature with engine and cooling conditions for four engines.

engine with a maximum spark-plug temperature approximately 50° F. higher than that of a Wright R–1820–G engine. The difference between the spark-plug and the average head temperatures for the Pratt & Whitney R–1535 engine is about 50° F. greater than for the Wright R–1820–G engine. Thus, the specification of the higher maximum spark-plug temperature for the Pratt & Whitney engine is equivalent to specifying equal average head temperatures for both engines.

The cooling-air velocities listed in the foregoing table and used in calculating the factor $\frac{I/v}{V\rho/\rho_0}$ in figure 18 were measured in the test-stand cooling duct. This velocity bears no relation to any velocity measured in flight and no comparison can be made between cooling in flight and on the test stand. This difficulty can be

avoided by measuring the cooling pressure drop and basing the correlation on an equation similar to (10a).

If equation (10b) is used for correlating cooling data in flight, it must be remembered that the velocity of the airplane in the low-speed range is an unreliable index of the air velocity between the cylinder fins as the effect of the propeller slipstream becomes important.

Figure 19 shows the percentage of brake horsepower required for cooling the 1340–H and the 1820–G cylinders at standard sea level plotted against the specific power output. The 1820–G cylinder was considered

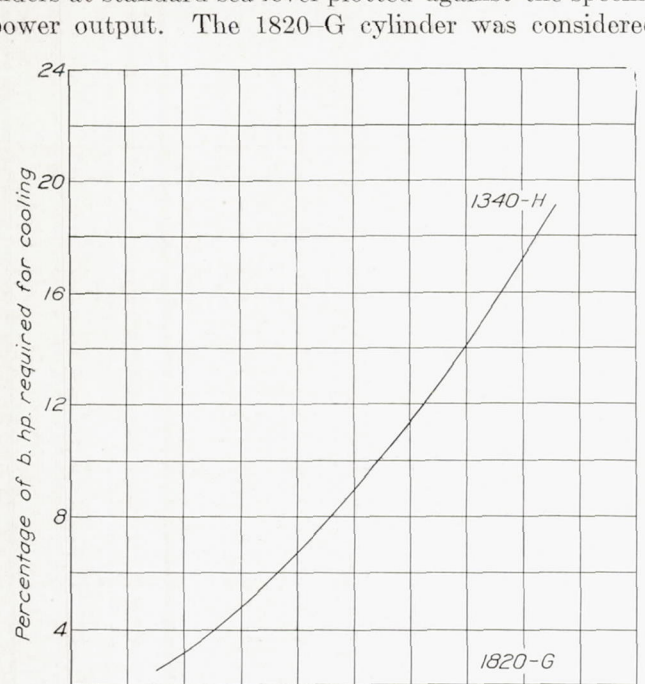

FIGURE 19.—Percentage of brake horsepower required for cooling by 1340–H and 1820–G cylinders.

adequately cooled when the maximum head temperature did not exceed 400° F. (average head temperature approximately 330° F.) and the cooling of the 1340–H cylinder was considered satisfactory when the maximum head temperature did not exceed 450° F. (average head temperature approximately 300° F.). The pressure drop required to maintain these temperatures was obtained from equation (33) for the head of the 1820–G cylinder and from a similar equation in reference 1 for the head of the 1340–H cylinder. The power required for cooling was calculated from the pressure drop and the volume of air, the volume of air being obtained from the calibration curves of each cylinder. (See fig. 3.) The power required to cool these engines in flight may be somewhat less than that shown in figure 19. The great difference shown in figure 19 between the power required for cooling the two cylinders illustrates the importance of providing adequate finning.

Effect of altitude on cylinder temperature.—It is of some interest to examine the variation in cylinder-head temperature with altitude for a typical air-cooled engine. A calibration curve of the Wright R–1820–22 engine with impeller-gear ratio of 7.14 : 1 was used for determining the variation of power with altitude. Equation (33) were assumed to apply to this engine. A constant value of T_g equal to 1,150° F. was used because only a small variation in T_g with reduction in back pressure is indicated by figure 11. The variation of atmospheric density and temperature with altitude was obtained from a table of standard altitude (reference 5).

Figure 20 shows the variation in average head temperature with altitude for level flight at full open throttle for various cowling-exit openings. The curves for constant exit opening are designated by the pressure drop across the engine in level flight at sea level. As the altitude is increased, the pressure drop, of course, decreases. The variation in pressure drop with altitude was obtained on the assumption that a constant proportion of the velocity head of the free air stream

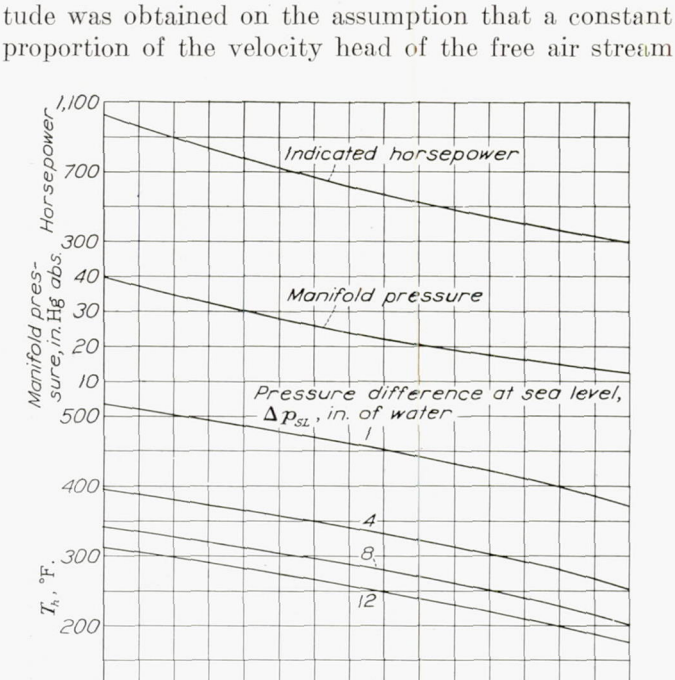

FIGURE 20.—Variation of head temperature of a Wright R–1820–22 engine with altitude for level flight at full open throttle (7.14:1 impeller ratio).

was maintained as pressure drop across the engine with a constant cowling-exit opening. The velocity head was calculated on the assumption that the airplane velocity varied directly as the cube root of the engine horsepower and inversely as the atmospheric density. The cylinder-head temperature is seen to decrease with altitude at full open throttle mainly because of the reduction in engine power.

If a supercharger is provided for maintaining a constant engine power over the range of altitudes considered, the temperature in level flight increases with

altitude, as seen in figure 21. The rate of temperature rise with altitude decreases as the size of the exit opening is increased or, in other words, as the temperature at sea level is decreased. With the lower head temperature, the reduction in atmospheric temperature with altitude has a greater effect on cooling because the percentage increase in temperature difference between the cylinder head and the cooling air becomes greater for a given change in cooling-air temperature. In these computations, the assumption is made that the charge temperature in the inlet manifold is held constant.

Constant charge temperature can, of course, be maintained by means of an adequate intercooler. At present, intercoolers are not provided with sufficient capacity for maintaining sea-level temperatures at

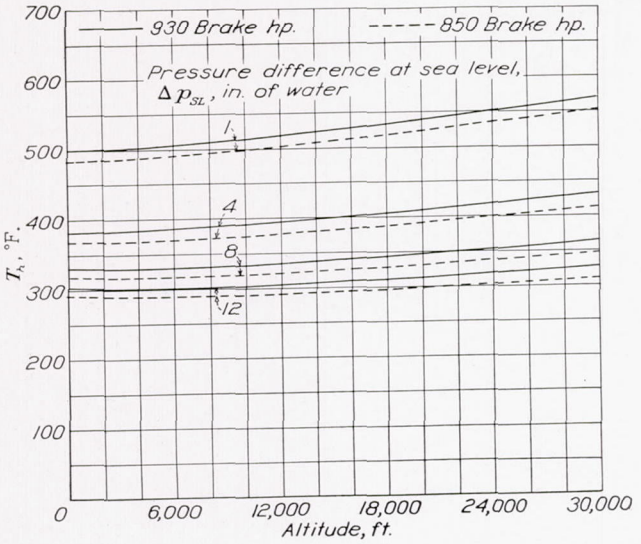

FIGURE 21.—Variation of head temperature of a Wright R–1820–22 engine with altitude for level flight. Horsepower constant.

altitude, and considerable heating of the inlet charge is experienced. The most serious consequence of high charge temperature is the increased tendency to detonate. When an engine is operating near the detonation condition, a 100° F. rise in charge temperature, for example, may cause a 9-percent decrease in permissible manifold pressure. The same increase in charge temperature will cause only a 15° F. rise in cylinder-head temperature for constant engine power if no detonation occurs. A much greater rise in cylinder-head temperature than 15° F. would result if detonation were encountered; the additional temperature rise must, however, be attributed to detonation rather than to the direct effect of charge temperature as it can be eliminated by increasing the octane number of the fuel.

The variation of the head temperature in climb at a constant indicated air speed and at full open throttle is shown in figure 22. The condition of constant indicated air speed established the relative velocities at the various altitudes. As before, the cooling pressure drop for a given exit opening was taken as a constant ratio of the velocity head of the free air stream. The curves of constant exit opening are designated by the values of the cooling pressure drops at sea level. These curves

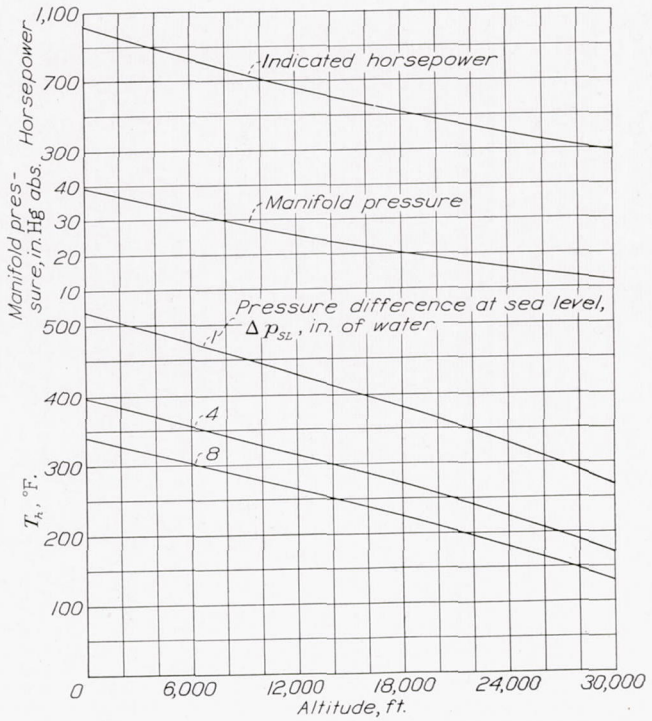

FIGURE 22.—Variation of equilibrium head temperature for a Wright R–1820–22 engine with altitude for climb at constant indicated air speed (7.14:1 impeller ratio).

again indicate a reduction in cylinder-head temperature with altitude, mainly because of the reduction in engine power. When the engine power is held constant, as seen from figure 23, a very slight increase in head

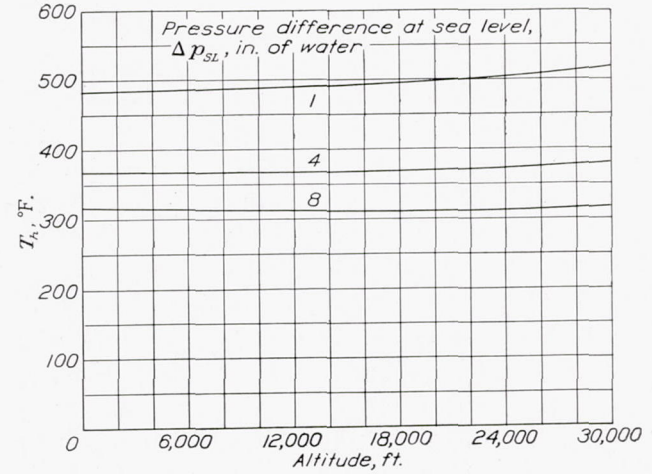

FIGURE 23.—Variation of equilibrium head temperature for a Wright R–1820–22 engine with altitude for climb at constant indicated air speed. Indicated horsepower constant.

temperature with altitude is obtained. As in the case of level flight, the assumption is made that the charge temperature remains constant with change in altitude and the remarks previously made also apply to the case of climb. The curves in figures 22 and 23 repre-

sent the equilibrium temperatures for the conditions existing at each altitude. In a rapid climb, considerable lag in the response of the cylinder temperature with the changing conditions is generally obtained.

Reference 2 shows that, when the engine or the cooling conditions were suddenly changed at time $t=0$ and thereafter held constant, the cylinder-head temperature would approach its new equilibrium value according to the equation (equation (11), reference 2)

$$T_{h_t}=T_h-(T_h-T_{h_0})\,e^{-\frac{At}{cM}}$$

where

$$A=Ka_0(\Delta p\rho/\rho_0)^m+\bar{B}a_1 I^{n'}$$

of 308° F. was attained. The curve of $1-e^{-0.606t'}$ is seen to represent these data with a fair degree of accuracy. With the preceding change in head temperature, the barrel temperature increased from 171° to 216° F. The factor $(T_{b_t}-T_{b_0})/(T_b-T_{b_0})$ for the barrel is also shown in figure 24.

In the second case, the engine was operated with an average head temperature of 226° F., an indicated horsepower of 35.2, and a cooling-air pressure drop of 11.8 inches of water. The pressure drop across the cylinder was suddenly decreased to 3.0 inches of water and the average cylinder-head temperature approached the new equilibrium temperature of 286° F. at a rate indicated

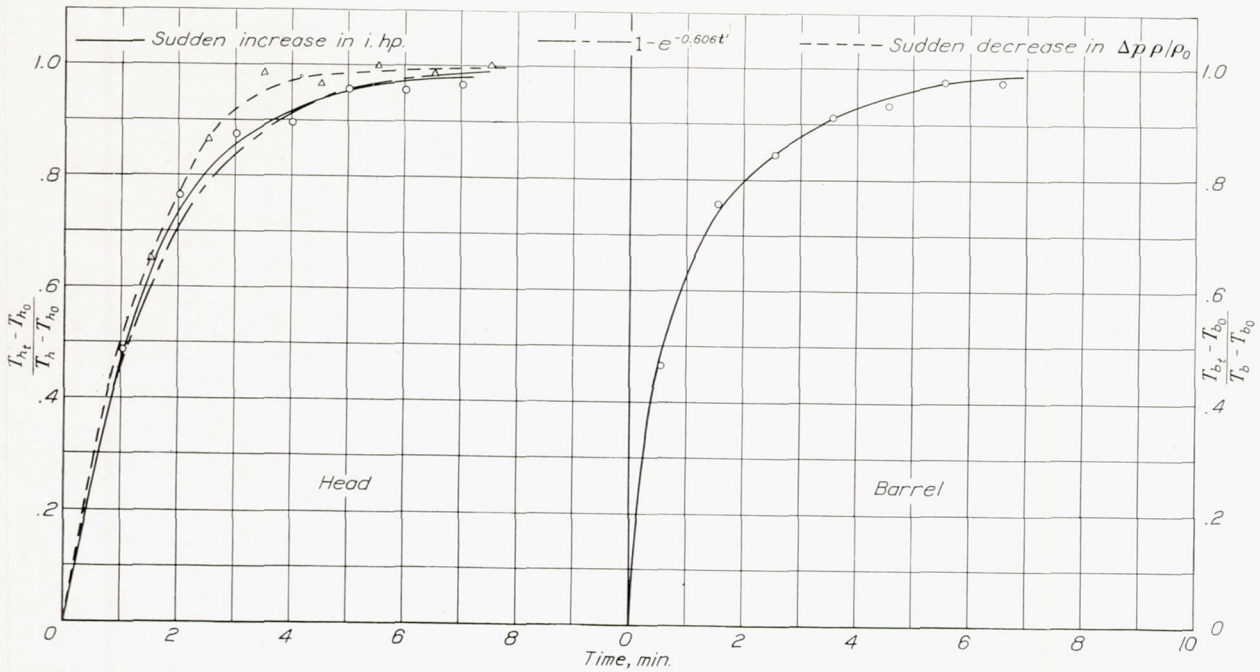

FIGURE 24.—Variation with time of the ratio of the change in temperature to the total change in temperature for a sudden change in engine operating conditions.

and the other symbols have the significance previously given. The terms in the foregoing equation may be rearranged as follows:

$$\frac{T_{h_t}-T_{h_0}}{T_h-T_{h_0}}=1-e^{-\frac{At}{cM}}$$

As t approaches infinity, the factor $(T_{h_t}-T_{h_0})/(T_h-T_{h_0})$ approaches 1. Figure 24 shows $(T_{h_t}-T_{h_0})/(T_h-T_{h_0})$ plotted against time for two cases. In the first case, the engine was operated at an average cylinder-head temperature of 220° F., an indicated horsepower of 34.9, and a cooling pressure drop of 8.0 inches of water. The sudden opening of the throttle increased the indicated horsepower to 64.2. The measured average cylinder-head temperature increased with time, as indicated in figure 24, until an equilibrium temperature

in figure 24. The curve for the barrel temperature has been omitted because the change in the cooling condition was insufficient to have an appreciable effect on barrel temperature. These curves show that, if a climb takes 4 minutes, the temperature of the head would increase, roughly, 90 percent of the difference between the final equilibrium temperature and the temperature at the start of the climb. Large differences in temperature between initial and final conditions might be obtained, for example, by suddenly going from a high forward speed into a steep climb and, in these cases, the cylinder temperatures for the first 4 or 5 minutes might differ considerably from the equilibrium temperature. The variation of engine power, cooling-air temperature, and mass flow with altitude that normally occur in climb tests introduces additional lag in cylinder-head temperature, and the difficulty of obtaining consistent data in climb is evident.

CONCLUSIONS

1. The theory previously developed and checked on two engine cylinders of the effect of engine and cooling conditions on average cylinder temperatures was further substantiated by data obtained on a cylinder from a Wright R–1820–G engine.

2. The methods presented for correlating and comparing cooling-test data obtained on the test stand and in flight both for individual points on the cylinder and for the entire cylinder are satisfactory when applied to data obtained on a number of service engines.

3. When the cooling pressure drop was suddenly increased and also when the throttle was suddenly opened, a time duration of approximately 4 minutes was required for the temperature rise to equal 90 percent of the total rise to equilibrium temperature.

LANGLEY MEMORIAL AERONAUTICAL LABORATORY,
NATIONAL ADVISORY COMMITTEE FOR AERONAUTICS,
LANGLEY FIELD, VA., *August 15, 1939.*

APPENDIX

TEMPERATURE AT INDIVIDUAL POINTS ON CYLINDER

THEORETICAL DISTRIBUTION OF TEMPERATURE AROUND THE CYLINDER

The previous analysis has been confined to a discussion of average head and barrel temperatures. The problem of the distribution of temperature around the cylinder is complicated by the introduction of a number of additional variables. An insight into the effect of some of the factors involved may be obtained from a consideration of the temperature distribution about a baffled finned cylinder containing a hot gas; the simplifying assumptions are made that the temperature of the gas in the cylinder, the local heat-transfer coefficient from the gas to the cylinder wall, and the local heat-transfer coefficient from the cylinder wall through the fins to the cooling air are constant with regard to distribution about the cylinder. By local heat-transfer coefficient is meant the coefficient based on the difference between the temperatures of the wall and the fluid in the vicinity of the point under discussion.

Let q_{0_x} represent the local heat-transfer coefficient from engine gas to cylinder wall and U_x represent the local heat-transfer coefficient from cylinder wall to cooling air. (The coefficient U_x is based on cylinder-wall temperature and area and includes the effect of conduction through the fins.)

The rate of heat transfer from the gas to a cylinder-wall surface of unit height and circumferential length dx is given by

$$dH_h=q_{0_x}(T_g-T_{h_x})dx \tag{11}$$

The rate of heat transfer from the same element of cylinder wall to the cooling air is given by

$$dH_h=U_x(T_{h_x}-T_{a_x})dx \tag{12}$$

The amount of heat carried away by the cooling air flowing over the element considered is

$$dH_h=c_p\frac{W_h}{2}dT_{a_x} \tag{13}$$

At equilibrium

$$q_{0_x}(T_g-T_{h_x})dx=U_x(T_{h_x}-T_{a_x})dx=c_p\frac{W_h}{2}dT_{a_x} \tag{14}$$

Let

$$\left.\begin{aligned} a&=\frac{q_{0_x}}{q_{0_x}+U_x}\\ \text{and}\qquad b&=\frac{U_x}{q_{0_x}+U_x}\end{aligned}\right\} \tag{15}$$

Then

$$T_{h_x}=aT_g+bT_{a_x} \tag{16}$$

$$c_pW_hdT_{a_x}=2U_xa(T_g-T_{a_x})dx$$

$$T_{a_x}-T_g=e^{-2U_xax/c_pW_h}\times\text{constant}$$

As $T_{a_x}=T_{a_1}$ (the inlet-air temperature) when $x=0$,

$$T_{a_x}=-(T_g-T_{a_1})e^{-2U_xax/c_pW_h}+T_g \tag{17}$$

The wall temperature is given by

$$T_{h_x}=aT_g+bT_g-b(T_g-T_{a_1})e^{-2U_xax/c_pW_h}$$

or

$$T_{h_x}=T_g-b(T_g-T_{a_1})e^{-2U_xax/c_pW_h} \tag{18}$$

The heat transferred per unit of time from the engine gas to the cylinder wall per unit of cylinder-wall area is then

$$\frac{dH_h}{dx}=bq_{0_x}(T_g-T_{a_1})e^{-2U_xax/c_pW_h} \tag{19}$$

The magnitude of the exponent $2U_xax/c_pW_h$ may be estimated in the following manner:

$$a=\frac{q_{0_x}}{q_{0_x}+U_x}=\frac{1}{1+\dfrac{U_x}{q_{0_x}}}=\frac{1}{1+\dfrac{T_g-T_{h_x}}{T_{h_x}-T_{a_x}}}=\frac{T_{h_x}-T_{a_x}}{T_g-T_{a_x}}$$

The heat dissipated per unit height of cylinder and length x_t is given approximately by

$$H_h=U_x(T_h-T_{a_{av}})x_t=c_p\frac{W_h}{2}(T_{a_0}-T_{a_1})$$

where x_t is the circumferential distance from the front to the rear of the cylinder T_{a_0} is the outlet cooling-air temperature. The quantity a may be represented approximately by

$$a=\frac{T_h-T_{a_{av}}}{T_g-T_{a_{av}}}$$

and $2U_xax_t/c_pW_h$ becomes $(T_{a_0}-T_{a_1})/(T_g-T_{a_{av}})$. The rise in cooling-air temperature across the head is generally of the order of 80° F. for conventional cooling, T_g is approximately 1,150° F., and the average cooling-air temperature is about 100° F. The value of $2U_xax_t/c_pW_h$ is thus approximately 0.08.

For the barrel, the rise in cooling-air temperature is generally 30° F., T_g is 600° F., and $T_{a_{av}}$ is 100° F. so that $2U_xax_t/c_pW_h$ is about 0.06. For these small

values of the exponent $2U_x a x_t/c_p W_h$, the value of $e^{-2U_x a x/c_p W_h}$ can be very closely represented by the first two terms of its series expansion. Equations (17), (18), and (19) may be written

$$T_{a_x}=T_{a_1}+\frac{2U_x a x}{c_p W_h(T_g-T_{a_1})} \tag{20}$$

$$T_{h_x}=T_g+\frac{2(T_g-T_{a_1})bU_x a x}{c_p W_h}-b(T_g-T_{a_1}) \tag{21}$$

and

$$\frac{dH_h}{dx}=bq_{0_x}(T_g-T_{a_1})\left(1-\frac{2U_x a x}{c_p W_h}\right) \tag{22}$$

Thus, the cooling-air temperature and the cylinder-wall temperatures increase practically linearly with circumferential distance around the cylinder and the heat transferred from the engine gases to the cylinder wall per unit of cylinder-wall area is almost constant, decreasing slightly toward the rear of the cylinder. Figure 25 shows the variation of T_{a_x}, T_{h_x}, and dH_h/dx calculated by the exact equations (17), (18), and (19) and by the approximate equations (20), (21), and (22) and plotted against angular position around the cylinder for the head and the barrel for a typical condition; the difference is seen to be small. The values of U_x and q_{0_x} were obtained from the test data.

THEORETICAL BASIS FOR CALCULATING AVERAGE HEAT-TRANSFER COEFFICIENTS

From equations (21) and (20), the difference between the average wall temperature and the average cooling-air temperature is

$$T_h-T_{a_{av}}=a(T_g-T_{a_1})\left(1-\frac{U_x a x_t}{c_p W_h}\right) \tag{23}$$

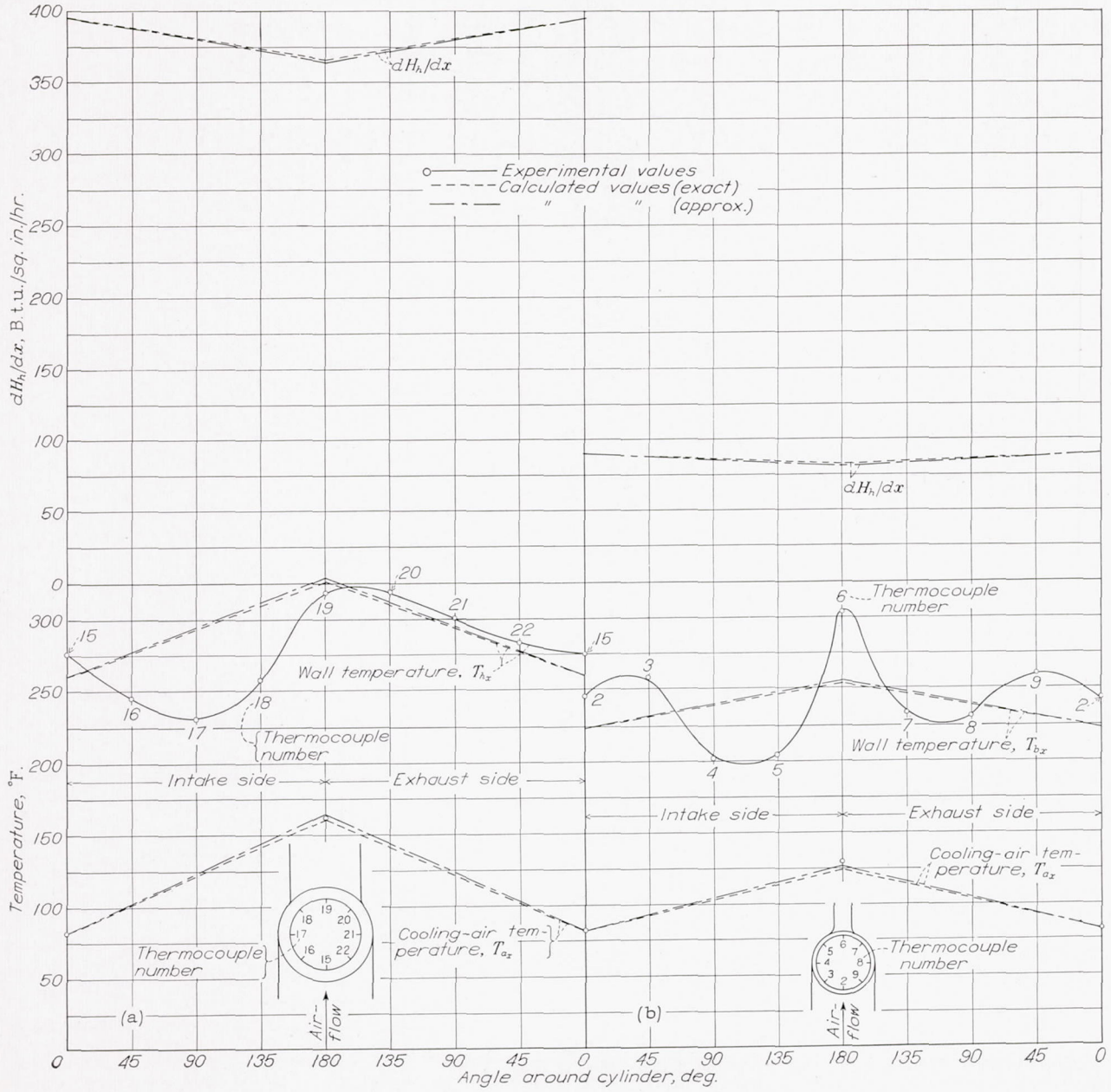

(a) Head. (b) Barrel.

FIGURE 25.—Temperature distribution around the cylinder.

From equation (22), the heat given off from the strip of cylinder wall of unit height and length x_t is

$$H_h=bq_{0_x}(T_g-T_{a_1})\left(x_t-\frac{U_x a x_t^2}{c_p W_h}\right) \tag{24}$$

But $bq_{0_x}=aU_x$

Dividing (24) by (23)

$$U_x=\frac{H_h}{x_t(T_h-T_{a_{av}})} \tag{25}$$

Thus, as indicated by the foregoing simplified case, the difference between the average wall temperature and the average air temperature instead of the logarithmic mean temperature difference should be used for obtaining the local heat-transfer coefficient. Even though in an engine the local heat-transfer coefficients vary around the cylinder, the foreoing method may be used to obtain an average of the local heat-transfer coefficients. The average cooling-air temperature in the present tests was taken as one-half the sum of the inlet and the outlet temperatures.

The over-all heat-transfer coefficient U based on the temperature difference between the average wall temperature and the inlet-air temperature is useful because the heat dissipated from the fins can be calculated from it without knowing the temperature rise of the air across the fins. The relation between U and U_x may be closely approximated by

$$U=U_x\left(1-\frac{U_x x_t}{c_p W_h}\right) \tag{26}$$

Inasmuch as U_x and W_h are functions only of $\Delta p\rho/\rho_0$, for a given finned cylinder, U is also a function only of $\Delta p\rho/\rho_0$.

The quantity q_0 is defined as

$$q_0=\frac{H_h}{x_t(T_g-T_h)}$$

From equation (21)

$$T_g-T_h=b(T_g-T_{a_1})\left(1-\frac{U_x a x_t}{c_p W_h}\right)$$

With this value of T_g-T_h and the expression for H_h given by equation (24), q_0 becomes

$$q_0=q_{0_x} \tag{26a}$$

Thus, the internal average heat-transfer coefficient for the theoretical finned cylinder is calculated from the average wall temperature.

METHOD FOR CORRELATING TEMPERATURES AT INDIVIDUAL POINTS ON CYLINDER BASED ON SIMPLIFYING ASSUMPTIONS

A relation useful for plotting temperature data at individual points on the cylinder will now be obtained. From equation (21), at a given point,

$$T_{h_x}-T_{a_1}=a(T_g-T_{a_1})\left(1+\frac{2bU_x x}{c_p W_h}\right)$$

and, from the same equation,

$$T_g-T_{h_x}=b(T_g-T_{a_1})\left(1-\frac{2U_x a x}{c_p W_h}\right)$$

$$\frac{T_{h_x}-T_{a_1}}{T_g-T_{h_x}}=\frac{a}{b}\frac{1+\frac{2bU_x x}{c_p W_h}}{1-\frac{2U_x a x}{c_p W_h}}$$

The value of $2U_x ax/c_p W_h$ was previously shown to be approximately 0.08 for the head and 0.06 for the barrel. Therefore

$$\frac{1}{1-\frac{2U_x a x}{c_p W_h}}$$

can be closely approximated by

$$1+\frac{2U_x a x}{c_p W_h}$$

as $a/b=q_{0_x}/U_x$ and $a+b=1$, the foregoing equation, neglecting second-order terms, becomes

$$\frac{U_x}{q_{0_x}}\frac{T_{h_x}-T_{a_1}}{T_g-T_{h_x}}=1+\frac{2U_x x}{c_p W_h} \tag{27}$$

Applying equations (26) and (26a)

$$\frac{U}{q_0}\frac{T_{h_x}-T_{a_1}}{T_g-T_{h_x}}=\left(1+\frac{2U_x x}{c_p W_h}\right)\left(1-\frac{U_x x_t}{c_p W_h}\right) \tag{28}$$

Inasmuch as U_x and W_h are functions of $\Delta p\rho/\rho_0$, the right-hand side of equation (28) for a given point x can be written as a function of $\Delta p\rho/\rho_0$,

$$\frac{U}{q_0}\frac{T_{h_x}-T_{a_1}}{T_g-T_{h_x}}=f_1(\Delta p\rho/\rho_0) \tag{29}$$

When $T_{h_x}=T_h$, then $f_1(\Delta p\rho/\rho_0)=1$. For other points, $f_1(\Delta p\rho/\rho_0)$ varies slightly with $\Delta p\rho/\rho_0$. Equation (29) may also be written

$$\frac{(\Delta p\rho/\rho_0)^m}{I^{n'}}\frac{T_{h_x}-T_{a_1}}{T_g-T_{h_x}}=f_2(\Delta p\rho/\rho_0) \tag{30}$$

Deviations of the observed cylinder-temperature distribution from the theoretical values as given by the previous equations are caused by the breaking down of the original assumptions. In the practical case, the temperature of the gas in the cylinder and the local heat-transfer coefficients U_x and q_{0_x} are not constant with regard to distribution around the cylinder. Higher values of T_g would be expected near the exhaust port than near the intake port as T_g is a weighted mean temperature over the cycle in which the weight associated with each temperature is the ratio of the instantaneous heat-transfer coefficient to the mean coefficient. In the vicinity of the intake port, the gas flow, and thus the heat-transfer coefficient, is high when the temperature is low, thus giving more weight on the average to

the low temperatures; whereas, near the exhaust port, the gas flow is high when the temperature is high.

The values of q_{0_x} should be highest near the ports because there the rate of gas flow is highest. The variation of U_x around the cylinder depends on the baffle and the fin design. The cooling of the front depends to some extent on the turbulence of the air in front of the engine. The cylinder baffles usually begin at the 90° position. The flow between the fins may or may not settle down to an equilibrium condition some distance after the start of the baffled portion, depending on the fin design. The flow breaks away from the rear of the cylinder and causes a region of low heat-transfer coefficient. Further variations are introduced by the changes in shape of the head and the changes in fin proportions and distribution. Considerable variation in U_x around the cylinder may thus be expected. The effect of the circumferential conduction of heat through the cylinder-wall metal from the hot to the cold portions of the cylinder has been omitted from the previous analysis. This effect would tend to some extent to equalize cylinder-wall temperature. When all these effects are considered, the equation for a given point on the cylinder still can be shown to be expressible in the form given by equation (29) or (30) with T_g replaced by T_{g_x}, the local gas temperature.

COMPARISON OF ACTUAL AND THEORETICAL DISTRIBUTION OF TEMPERATURE AROUND CYLINDER

Figure 25 (a) shows the variation in measured temperature around the head of the 1820–G cylinder compared with calculated values obtained from equations (18) and (21) for a theoretical cylinder having the same diameter, average fin dimensions, cylinder-wall area, and air flow as the head. The locations of the thermocouples noted in figure 25 are shown in figure 1. The calculated cylinder temperature increases practically linearly from front to rear because of the increase in cooling-air temperature around the cylinder (fig. 25). It is recalled that, when the calculated values were obtained, a uniform heat-transfer coefficient was assumed around the head. In the case of the engine, an increase in cylinder temperature from front to rear also occurs but superimposed on this rise are certain other effects. On the intake-port side, a considerable drop in actual temperature below the calculated curve and, on the exhaust side, an increase above the calculated curve appears. These differences are obviously caused by the cooling effect of the incoming charge on the intake side and the heating effect of the exhaust gases on the exhaust side.

Figure 25 (b) shows a similar comparison between calculated and experimental temperature distribution for the barrel. The experimental curves oscillate about the calculated curve as a mean. The cooling effect of the intake charge and the heating effect of the exhaust gas are also evident on the barrel but to a lesser degree than on the head. A considerable increase in temperature at the rear of the cylinder is also noted. This increase is caused by breakaway of the flow from the rear of the cylinder resulting in a large reduction in heat-transfer coefficient. The low heat-transfer coefficient at the front of the cylinder can be attributed to the fact that the velocity of the air approaching the front of the cylinder is low, as seen from the diagram of the duct in figure 25, and the flow is nonturbulent. In the case of an engine installed in a cowling, although the flow area at the front of the cylinders is large, considerable large-scale turbulence exists in the flow, which reduces the temperatures in this region. The high temperatures at the front and the rear of the head are noted in figure 25 (a). These curves indicate that a simplified analysis, which takes into consideration only the rise in temperature of the cooling air, is insufficiently accurate for predicting temperature distributions around an engine cylinder. An analysis of this type is of some interest, however, in bringing out the effects of the other important factors.

REFERENCES

1. Pinkel, Benjamin: Heat-Transfer Processes in Air-Cooled Engine Cylinders. T. R. No. 612, N. A. C. A., 1938.
2. Schey, Oscar W., Pinkel, Benjamin, and Ellerbrock, Herman H., Jr.: Correction of Temperatures of Air-Cooled Engine Cylinders for Variation in Engine and Cooling Conditions. T. R. No. 645, N. A. C. A., 1938.
3. Ellerbrock, Herman H., Jr., and Biermann, Arnold E.: Surface Heat-Transfer Coefficients of Finned Cylinders. T. R. No. 676, N. A. C. A., 1939.
4. Schey, Oscar W., and Pinkel, Benjamin: Effect of Several Factors on the Cooling of a Radial Engine in Flight. T. N. No. 584, N. A. C. A., 1936.
5. Diehl, Walter S.: Standard Atmosphere—Tables and Data. T. R. No. 218, N. A. C. A., 1925.

U. S. GOVERNMENT PRINTING OFFICE: 1940

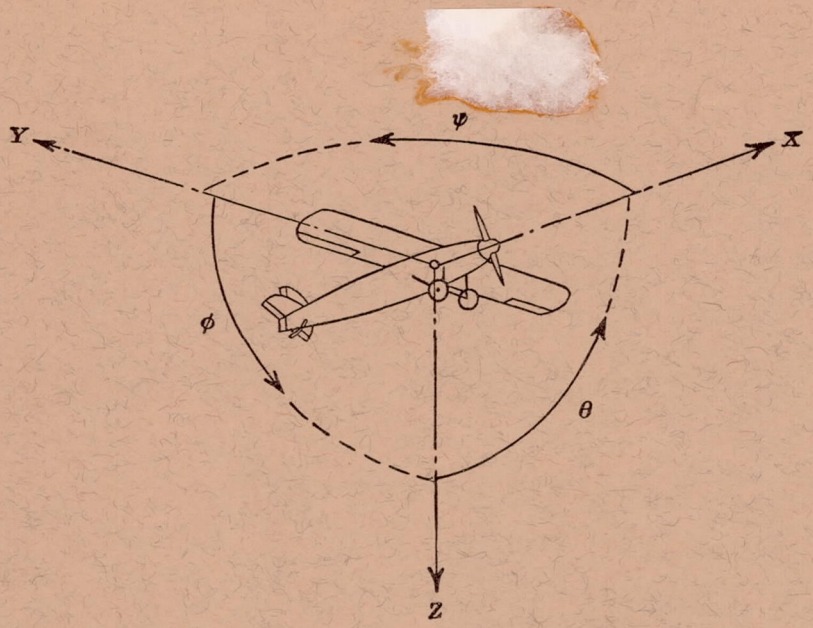

Positive directions of axes and angles (forces and moments) are shown by arrows

Axis		Force (parallel to axis) symbol	Moment about axis			Angle		Velocities	
Designation	Symbol		Designation	Symbol	Positive direction	Designation	Symbol	Linear (component along axis)	Angular
Longitudinal	X	X	Rolling	L	$Y \longrightarrow Z$	Roll	ϕ	u	p
Lateral	Y	Y	Pitching	M	$Z \longrightarrow X$	Pitch	θ	v	q
Normal	Z	Z	Yawing	N	$X \longrightarrow Y$	Yaw	ψ	w	r

Absolute coefficients of moment

$C_l = \frac{L}{qbS}$ (rolling) $\quad C_m = \frac{M}{qcS}$ (pitching) $\quad C_n = \frac{N}{qbS}$ (yawing)

Angle of set of control surface (relative to neutral position), δ. (Indicate surface by proper subscript.)

4. PROPELLER SYMBOLS

D, Diameter
p, Geometric pitch
p/D, Pitch ratio
V', Inflow velocity
V_s, Slipstream velocity
T, Thrust, absolute coefficient $C_T = \frac{T}{\rho n^2 D^4}$
Q, Torque, absolute coefficient $C_Q = \frac{Q}{\rho n^2 D^5}$
P, Power, absolute coefficient $C_P = \frac{P}{\rho n^3 D^5}$
C_s, Speed-power coefficient $= \sqrt[5]{\frac{\rho V^5}{P n^2}}$
η, Efficiency
n, Revolutions per second, r.p.s.
Φ, Effective helix angle $= \tan^{-1}\left(\frac{V}{2\pi r n}\right)$

5. NUMERICAL RELATIONS

1 hp.=76.04 kg-m/s=550 ft-lb./sec.
1 metric horsepower=1.0132 hp.
1 m.p.h.=0.4470 m.p.s.
1 m.p.s.=2.2369 m.p.h.
1 lb.=0.4536 kg.
1 kg=2.2046 lb.
1 mi.=1,609.35 m=5,280 ft.
1 m=3.2808 ft.